united nations educational, scientific and cultural organization

international atomic energy agency

abdus salam
international centre for theoretical physics

SMR 1232 - 13

XII WORKSHOP ON
STRONGLY CORRELATED ELECTRON SYSTEMS

17 - 28 July 2000

SCANNING SQUID MICROSCOPY
AND SUSCEPTOMETRY

Kathryn MOLER
Stanford University - LAM - Dept. of Applied Physics
94305-4045 Stanford, U.S.A.

These are preliminary lecture notes, intended only for distribution to participants.

strada costiera, 11 - 34014 trieste italy - tel. +39 0402240111 fax +39 040224163 - sci_info@ictp.trieste.it - www.ictp.trieste.it

Scanning SQUID microscopy and susceptometry

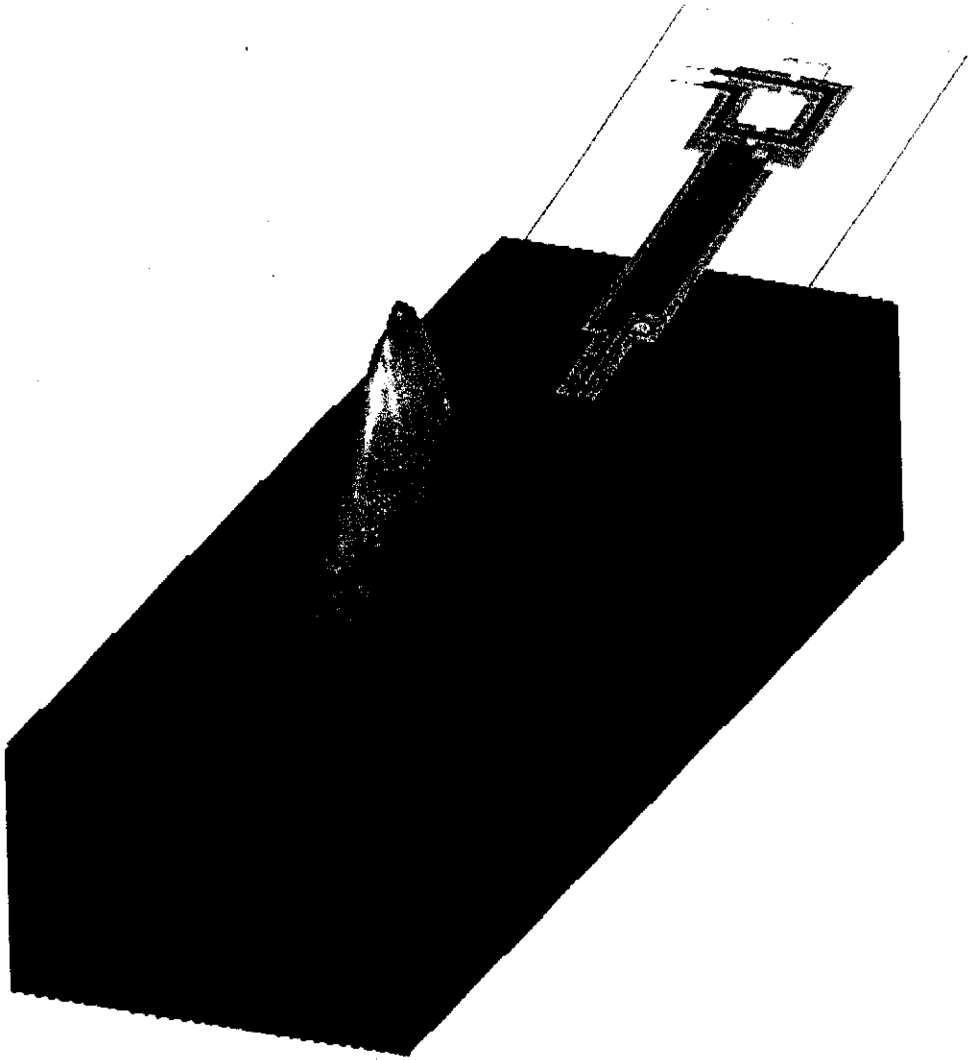

COLLABORATORS

IBM J.R. Kirtley, C.C. Tsuei, M. Ketchen, M. Bhushan

Argonne T.W. Li, M. Xu, D. Hinks
$Tl_2Ba_2CuO_{6+\delta}$

Groningen N. Kolesnikov, D. van der Marel, A. Tsvetkov
$Tl_2Ba_2CuO_{6+\delta}$

Caen G. Villard, A. Maignan
$(Hg, Cu)Ba_2CuO_{4+\delta}$

Tokyo M. Nohara, H. Takagi
$La_{2-x}Sr_xCuO_4$

ISU/Ames V. Kogan, J. Clem
I.L.J.V. Theory

Princeton N.P. Ong, P.W. Anderson, P. Chaikin

Stanford P. Bjornsson, B. Gardner,
E. Straver, J. Wynn

OUTLINE

Scanning SQUID Microscopy

Josephson Vortices in YBCO

- $\frac{1}{2}\Phi_0(T)$ in tricrystals
- $\lambda_J(T)$

Interlayer Josephson Vortices

- λ_c and interlayer tunneling
- Inter Layer Tunneling (ILT)

Scanning SQUID Susceptometry

Scanning SQUID Microscopy

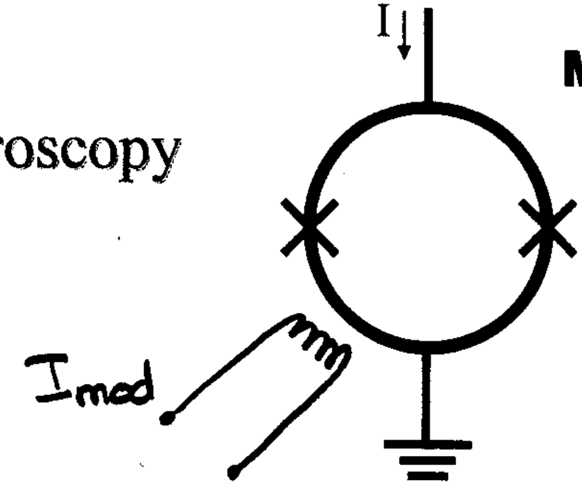

Magnetic flux

$$\Phi = \int \vec{B} \cdot d\vec{a}$$

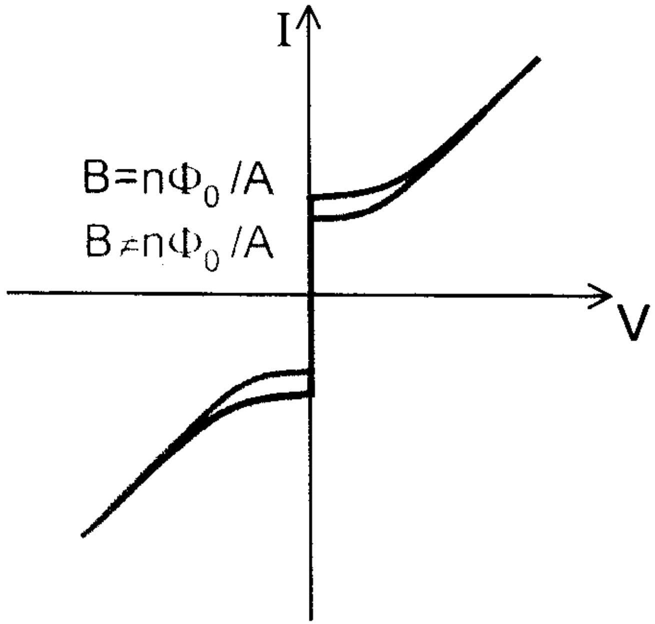

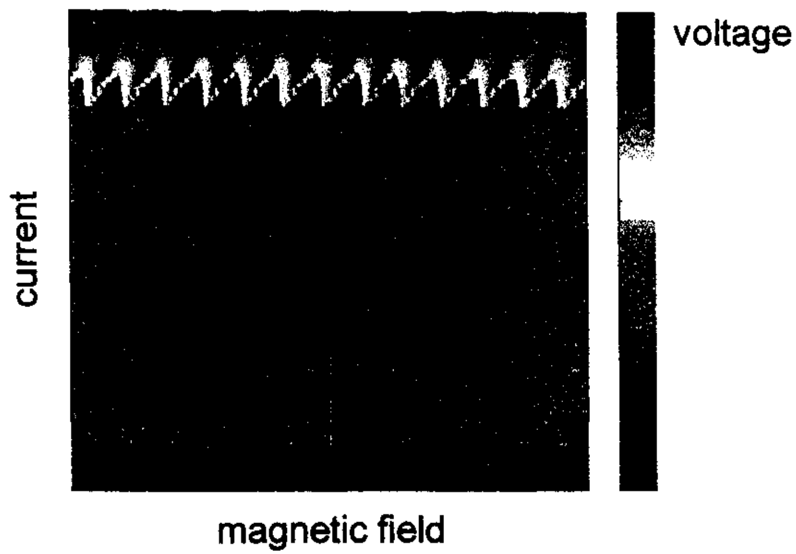

SQUID characterization:
Brian Gardner, Jennifer Hsieh

Scannable SQUID

schematic

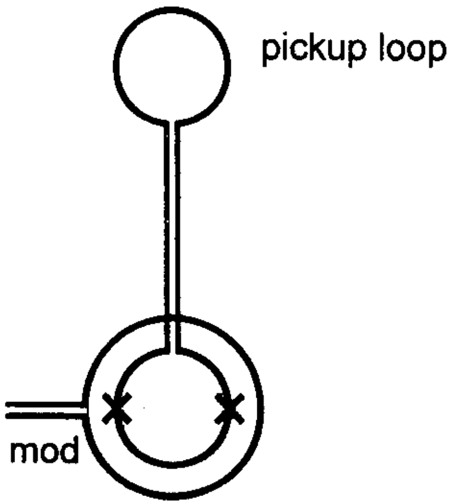

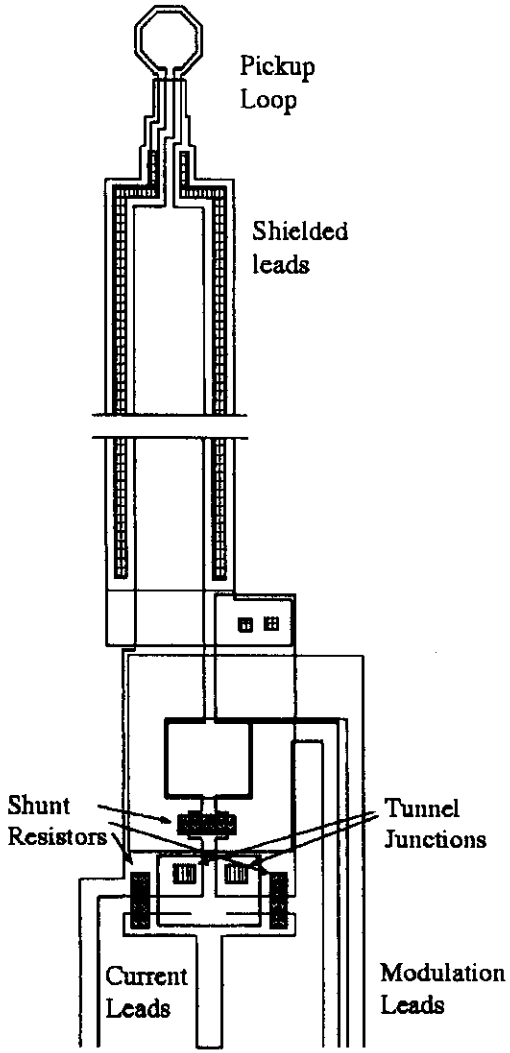

pickup loop designs

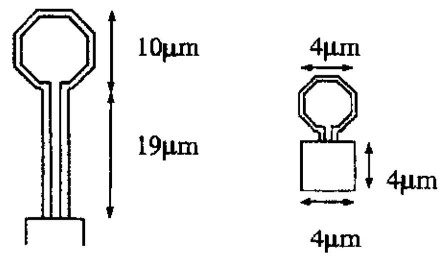

Scanning Something-on-a-Chip Microscopy

Measure total flux through pickup loop

$$\Phi_s = \int \vec{B} \bullet d\vec{a}$$

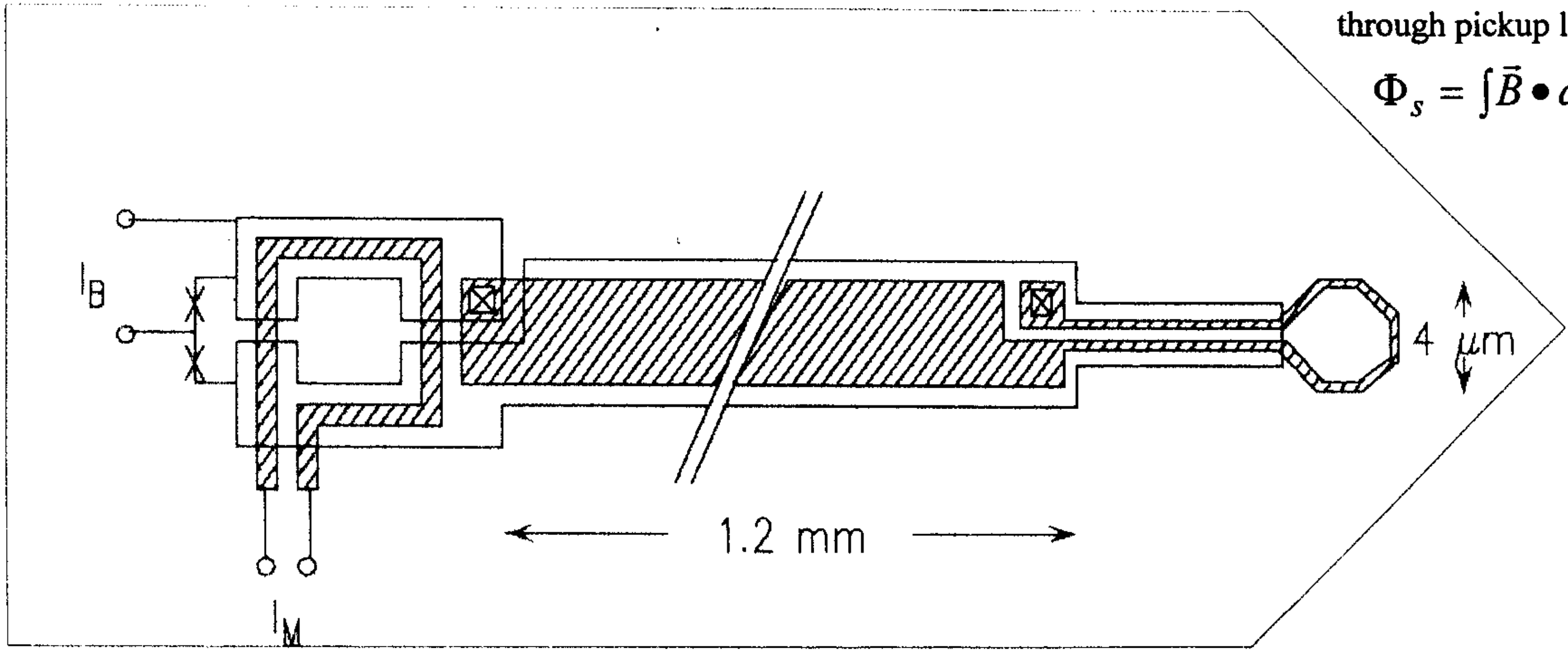

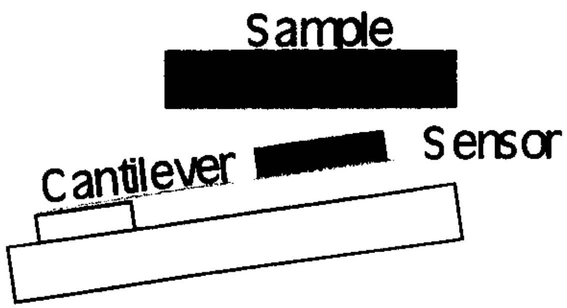

Sample up to 150 K
cm scan range

IBM Scanning SQUID Microscope:
Variable sample temperature mechanical scanner

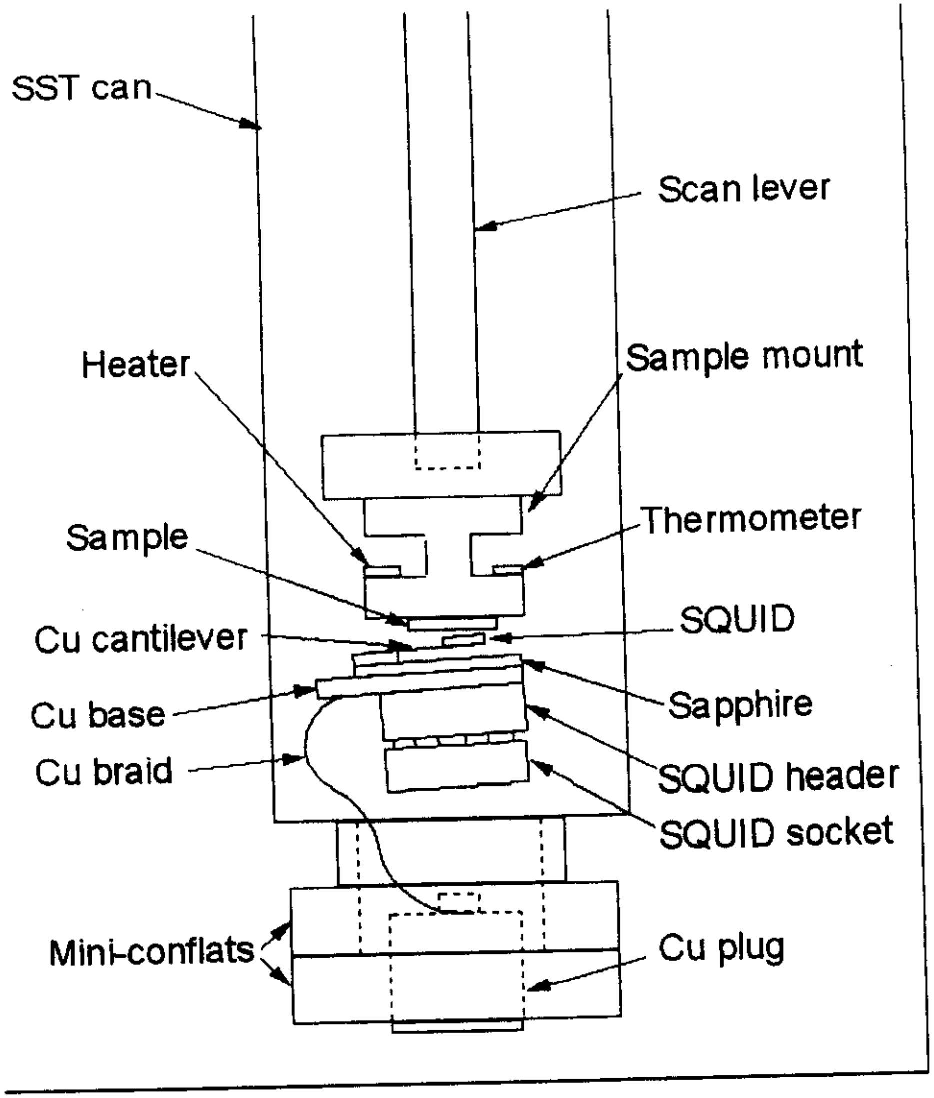

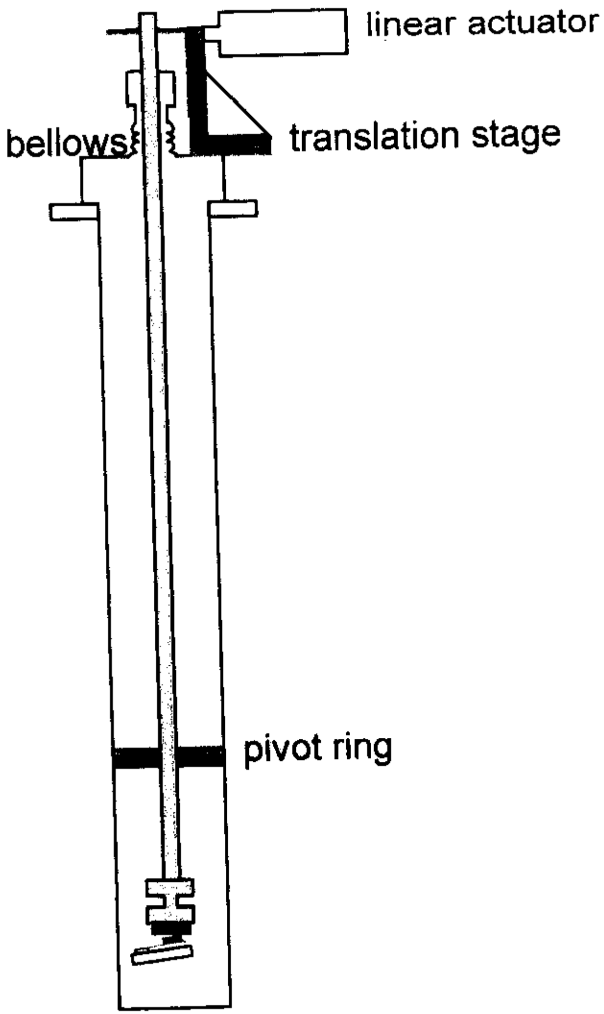

Types of Josephson vortices

Josephson vortex

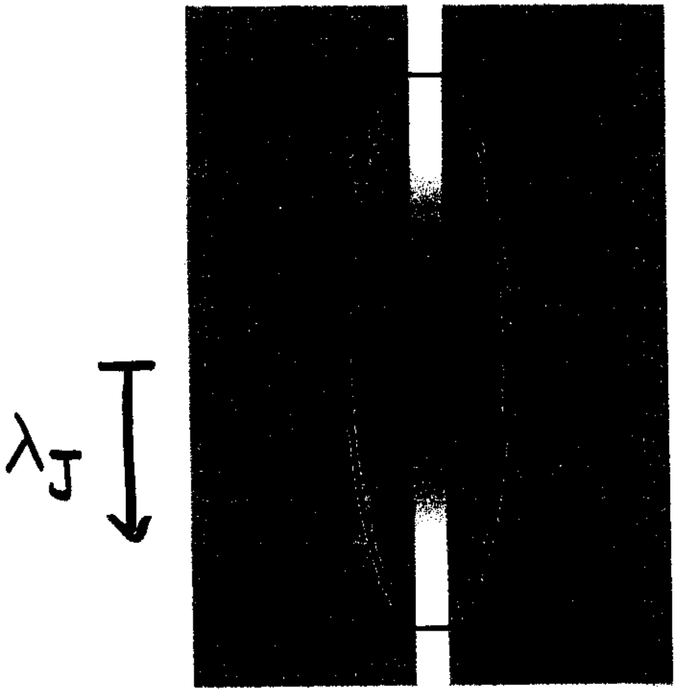

$$b_z(0,y)=\frac{4\pi\Phi_0}{d\lambda_J}\operatorname{sech}(y/\lambda_J)$$

Interlayer Josephson vortex

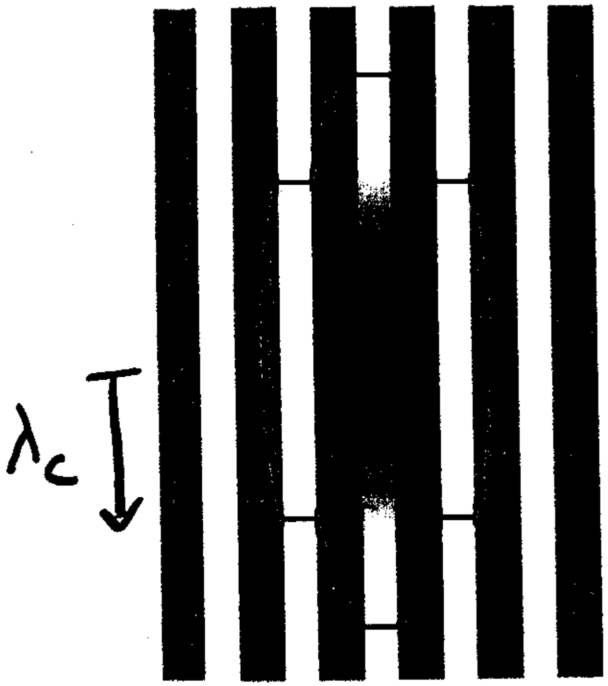

$$b_z(x,y)=\frac{\Phi_0}{2\pi\lambda_{ab}\lambda_c}\mathrm{K}_0(\tilde{R})$$

$$\tilde{R}=\sqrt{\left(s/2\lambda_{ab}\right)^2+\left(x/\lambda_{ab}\right)^2+\left(y/2\lambda_c\right)^2}$$

Lawrence & Doniach 1971
Coffey & Clem 1990

Half-Integral Flux Quantization

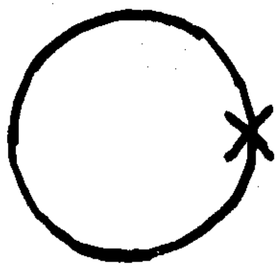

J.J.

$j = j_c \sin \Delta\phi$

$\Phi = n \Phi_0$

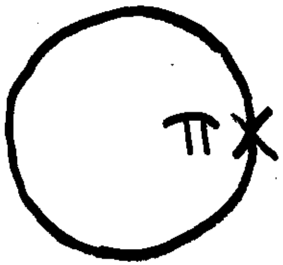

π junction

$j = -j_c \sin \Delta\phi$

$\Phi = (n + \frac{1}{2}) \Phi_0$

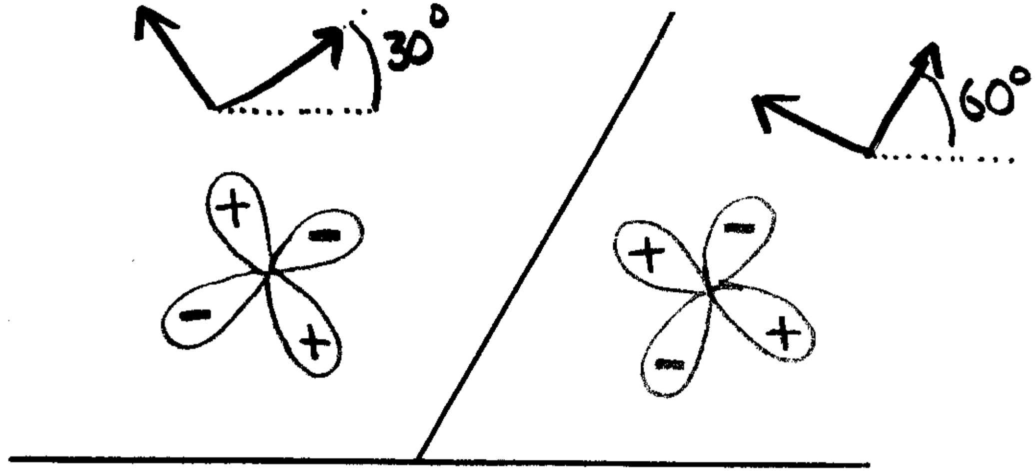

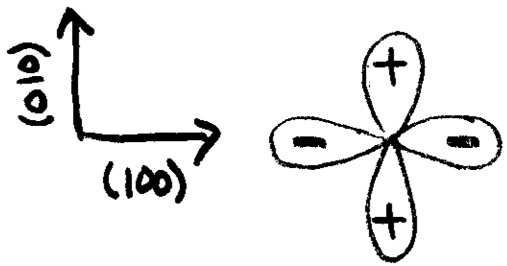

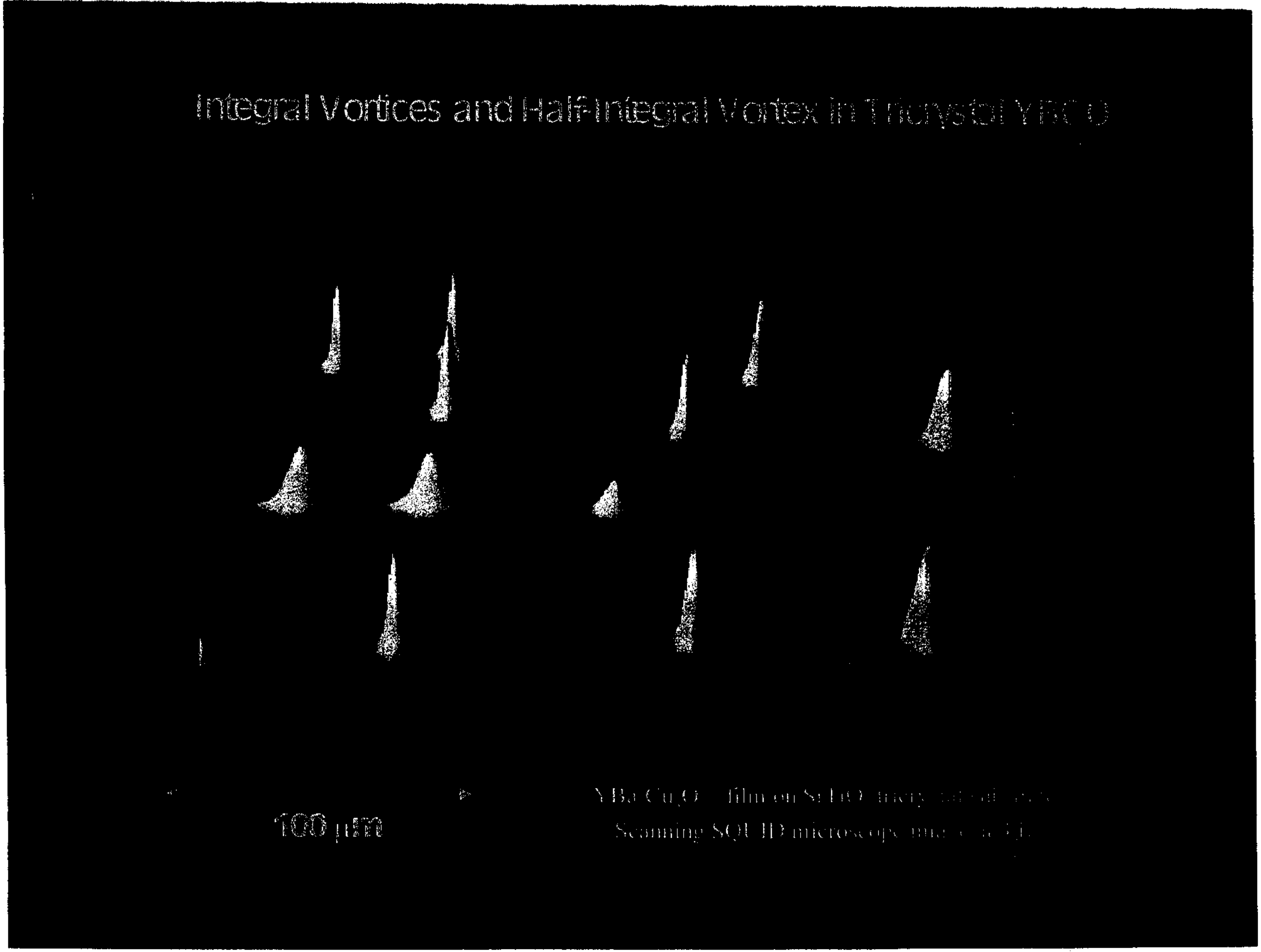
Integral Vortices and Half-Integral Vortex in Tricrystal YBCO
100 μm
film on
Scanning SQUID microscope

Temperature dependence of the half-integral flux quantum in YBCO

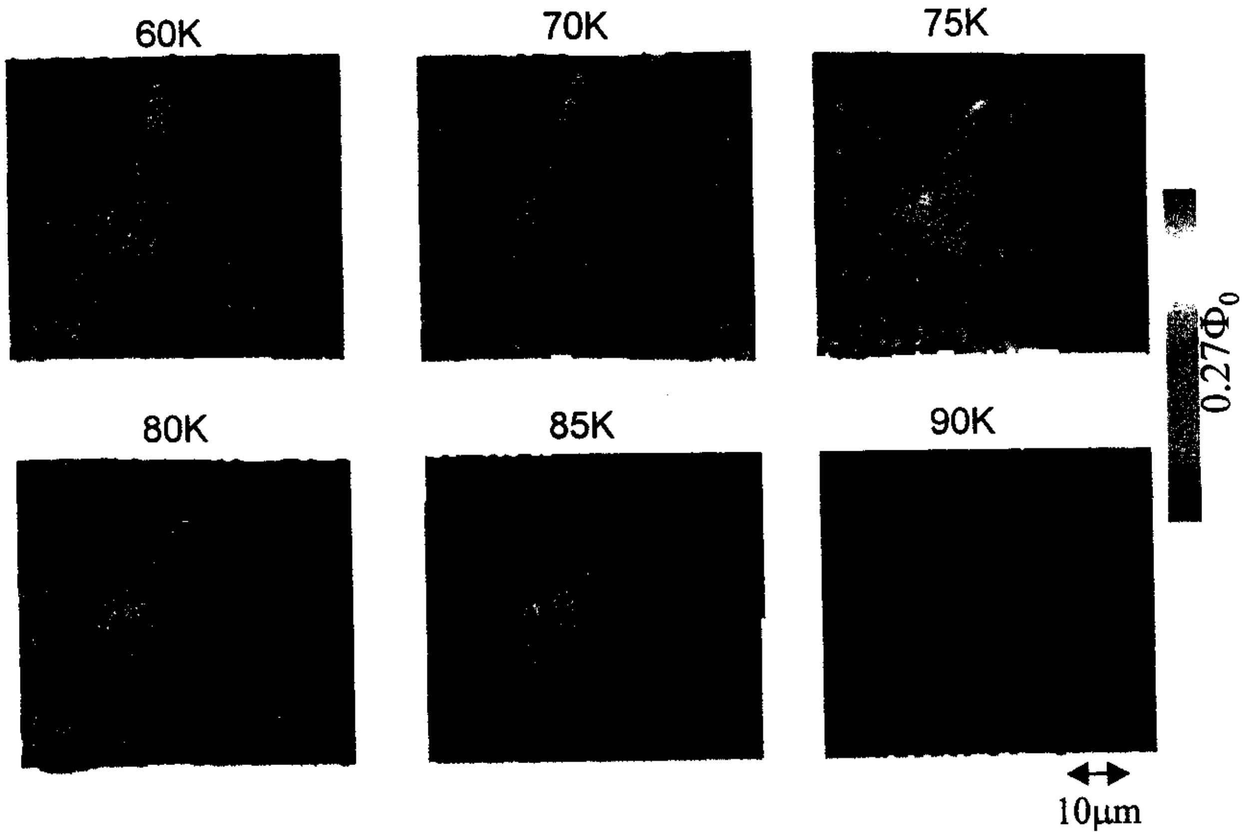

$\Phi_{trixtal} = \frac{\Phi_0}{2}$

for $0.4K \leq T \leq 88K$

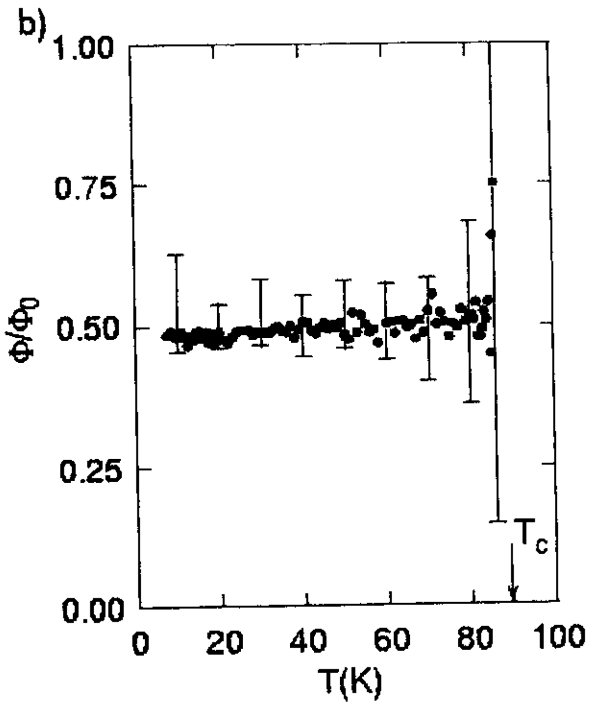

Kirtley, Tsuei, and Moler
1999

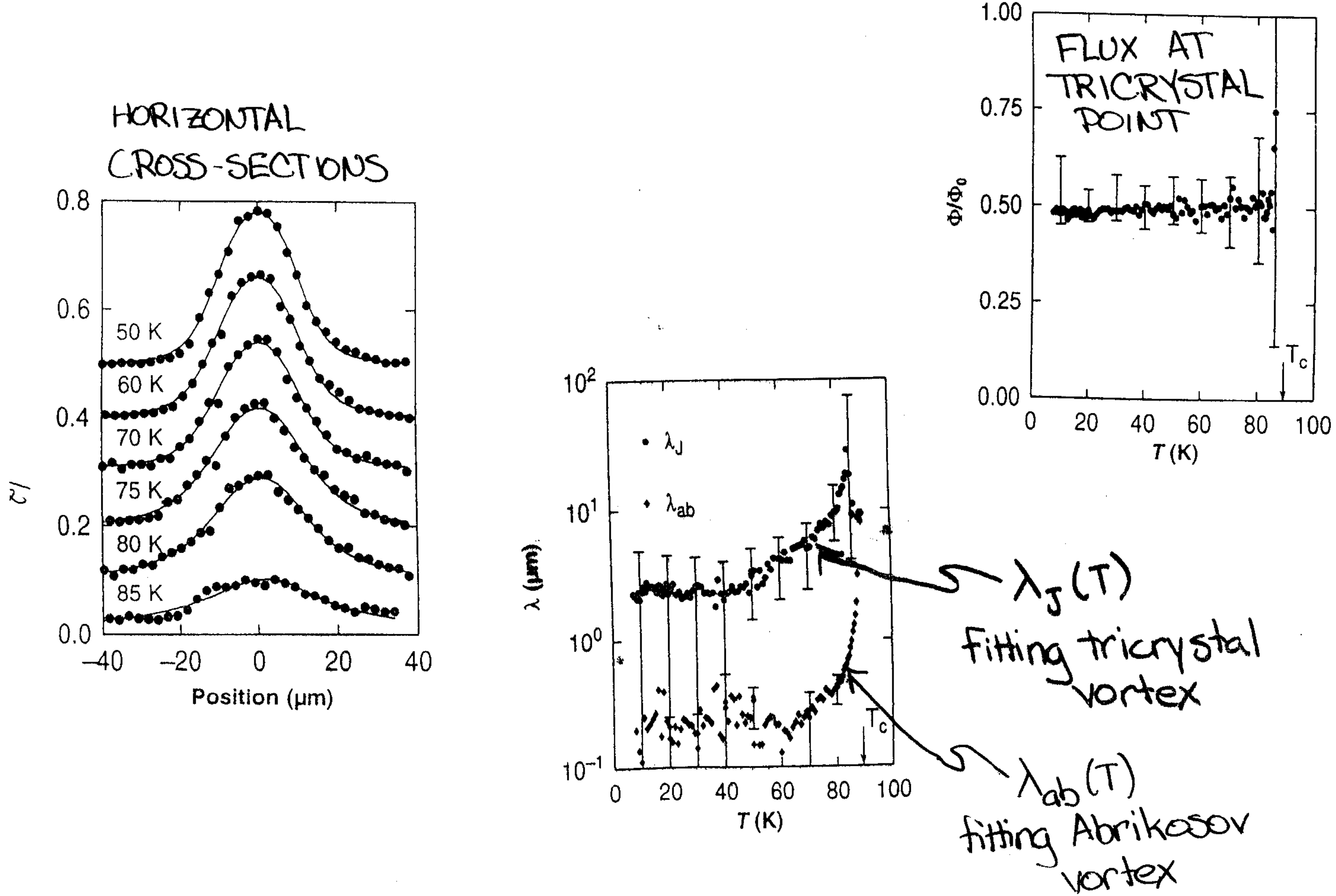

HORIZONTAL CROSS-SECTIONS
50 K
60 K
70 K
75 K
80 K
85 K
Position (μm)
λ_J
λ_ab
λ (μm)
T (K)
T_c
λ_J (T)
fitting tricrystal vortex
λ_ab (T)
fitting Abrikosov vortex
FLUX AT TRICRYSTAL POINT
Φ/Φ_0
T (K)
T_c

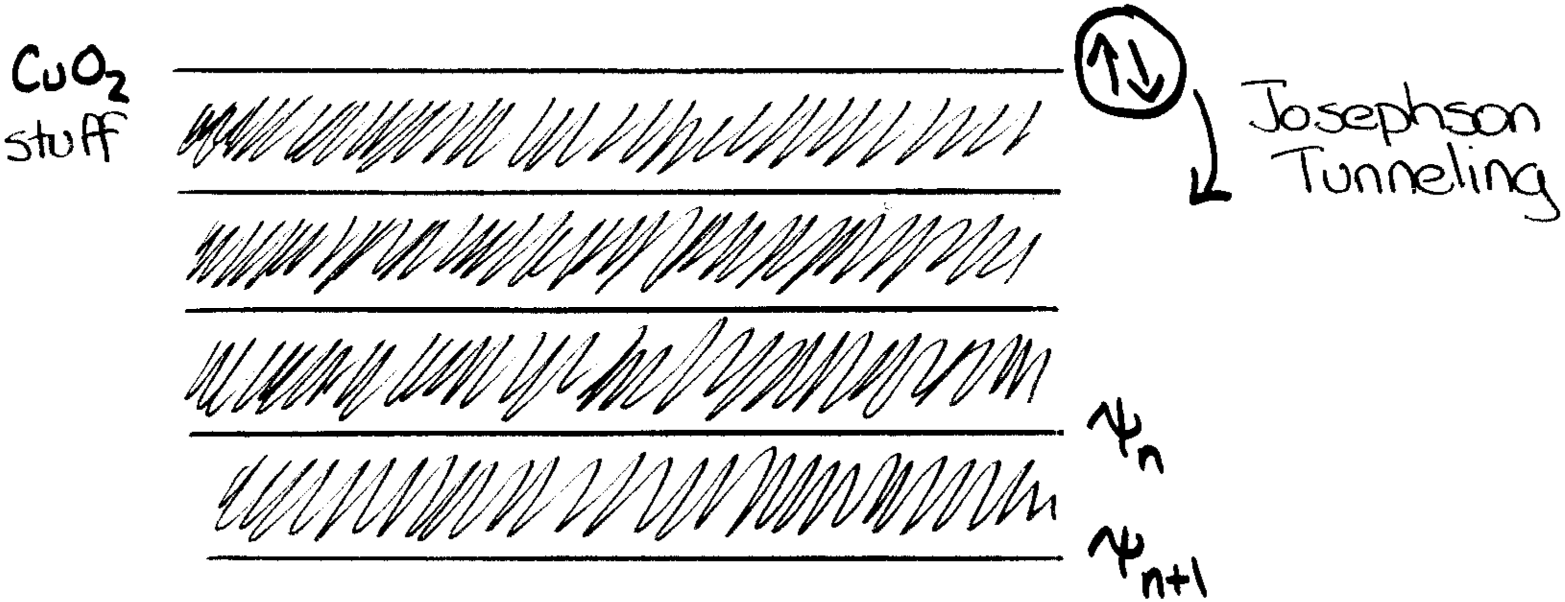

Lawrence-Doniach Model

Intrinsic Tunneling in $Bi_2Sr_2CaCu_2O_{8+x}$ Mesas

10 layers 3.5μ × 7.5μ

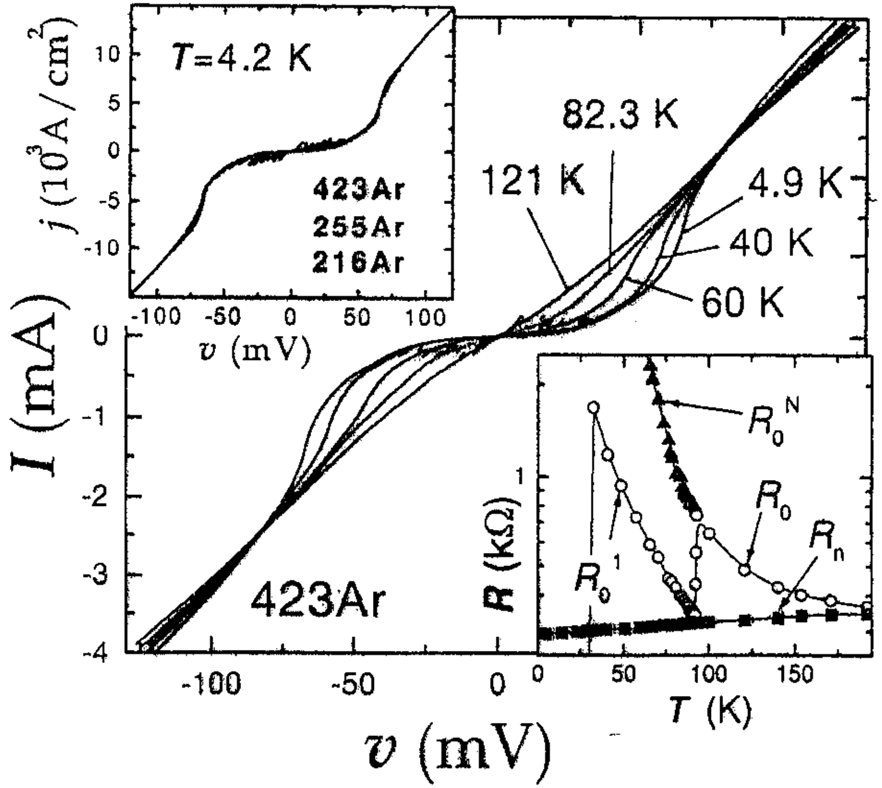

FIG. 1. I-υ curves for the 423Ar mesa at different T. Top inset shows normalized I-V curves at $T = 4.2$ K for three different mesas. Bottom inset shows in the logarithmic scale temperature dependencies of the zero bias resistance R_0 (open circles), large bias resistance R_n (solid squares) and the total subgap resistance R_0^N (solid triangles).

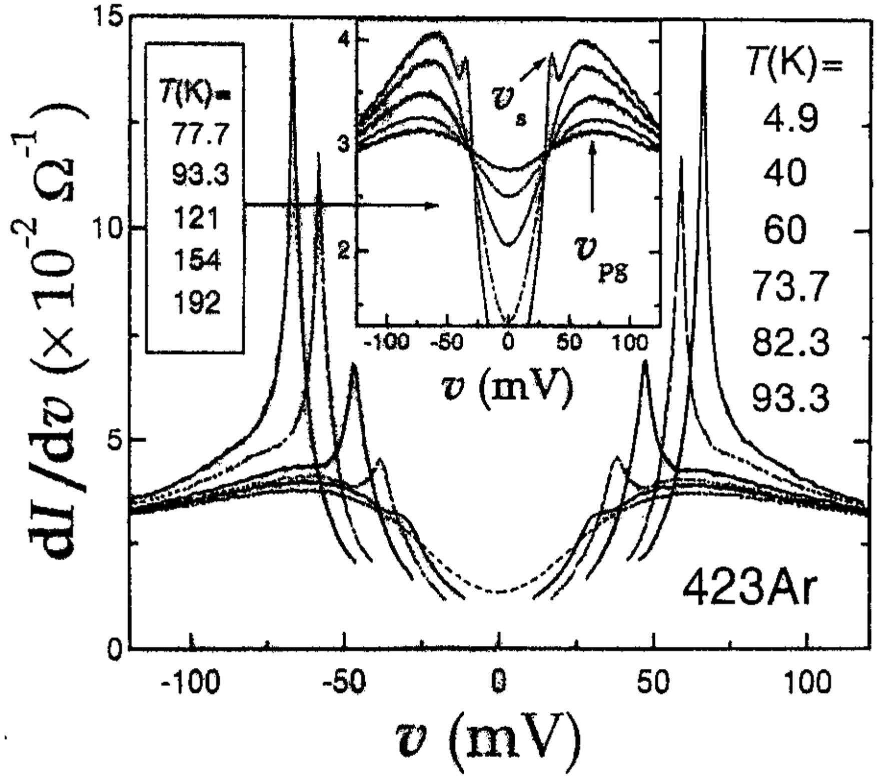

FIG. 2. Dynamic conductance, $\sigma(\upsilon)$, at different temperatures for 423Ar mesa. Inset shows detailed curves for high T. Coexistence of the superconducting peak, υ_s, and the pseudogap hump, υ_{pg}, is clearly visible at $T = 77.7$ K.

Krasnov Yurgens Winkler Delsing Claeson 2000

Josephson Plasma Resonance in $La_{2-x}Sr_xCuO_4$

Uchida, Tamasaku, and Tajima

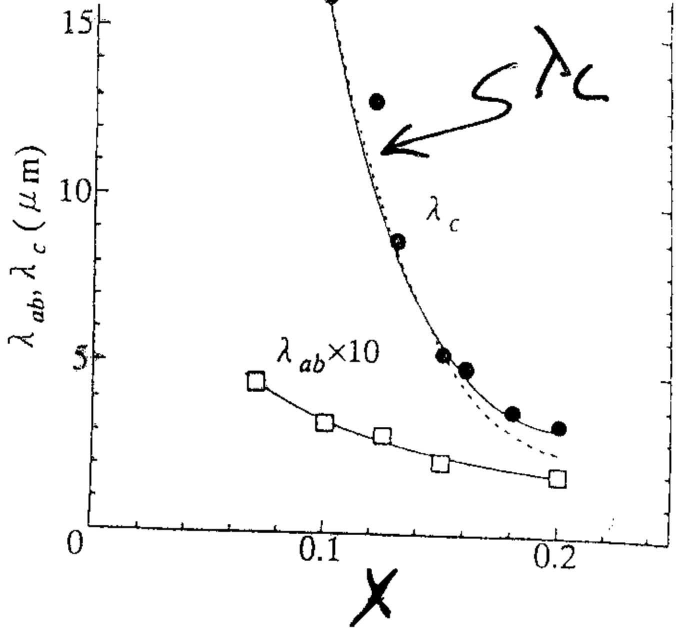

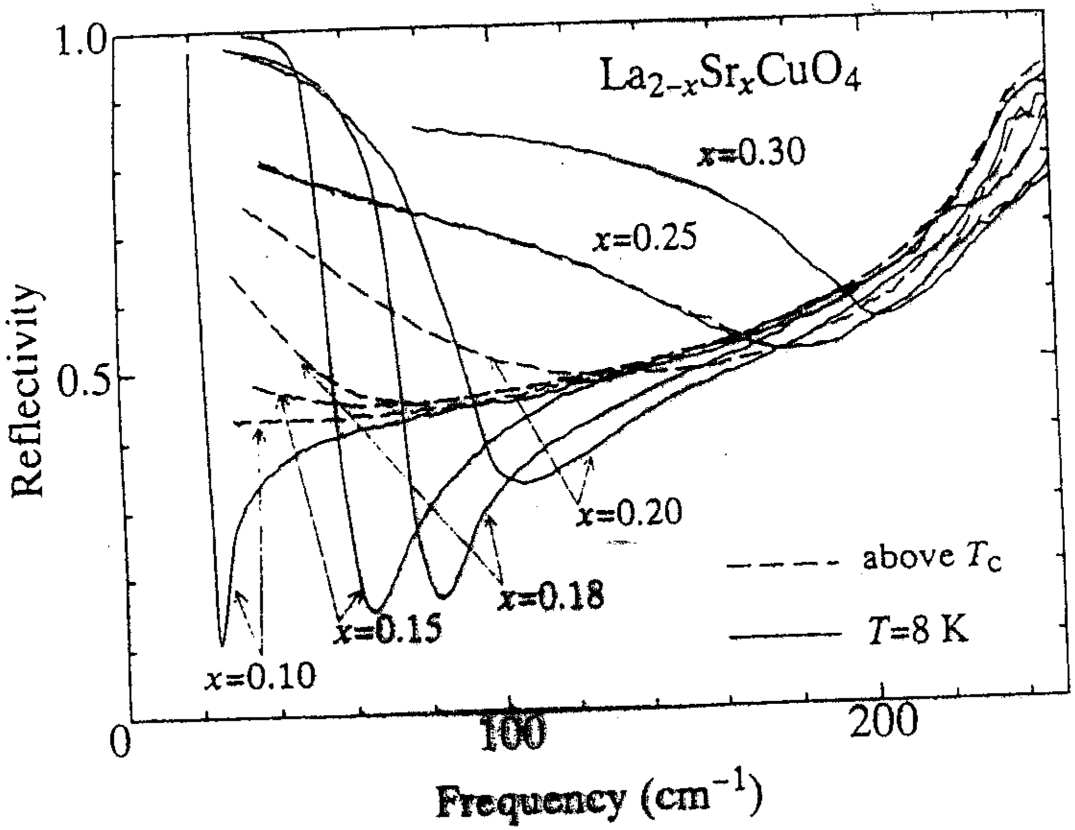

$$\omega_J = \frac{c}{\sqrt{\varepsilon}\,\lambda_c}$$

Ambegaokar-Baratoff model

applied to c-axis tunneling

$$\lambda_c = \sqrt{\frac{c\Phi_0}{8\pi^2 s J_0}}$$

Ambegaokar-Baratoff

$$J_0 = \frac{\pi\Delta_0}{2e\rho_{c,n}}$$

<u>problems</u>

- what's $\rho_{c,n}(T=4K, H\approx 0)$?
- anisotropic gap
- effective mass

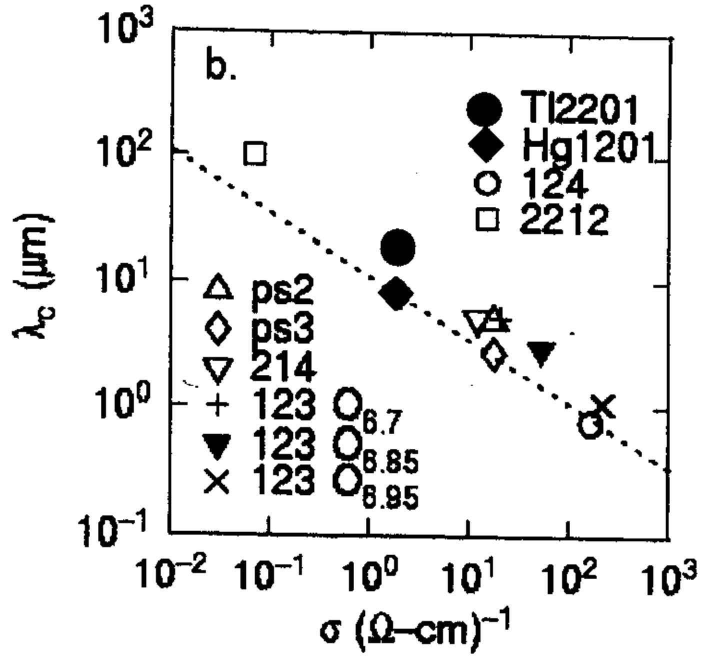

Basov 1994

Inter-Layer Tunneling Model*

J.W. Wheatley, T. Hsu, P.W. Anderson, 1988.
S. Chakravarty, A. Subdø, P.W. Anderson, S. Strong, 1993.

*** The ILT mechanism should not be confused with interlayer tunneling.**

Experimental test as formulated by A.J. Leggett 1996
(motivated by Groningen experiment)

$$\boxed{\lambda_c = \frac{\lambda_{ILT}}{2\eta^{1/2}}} \qquad \text{where} \qquad \lambda_{ILT} = \sqrt{\frac{mc^2}{E_c}\frac{a_0 A}{4\pi d}}$$

η — **fraction of condensation energy which comes from kinetic energy savings**

Single-layer high-Tc materials make the most straightforward test

Tl-2201 $\lambda_{ILT} \approx 1\ \mu m$
Hg-1201 $\lambda_{ILT} \approx 1\ \mu m$
LSCO $\lambda_{ILT} \approx 3\ \mu m$

bilayer

Josephson plasma frequency $\omega_p = \dfrac{c}{\lambda_c}$

van der Marel and coworkers 1995 Tl-2201 $\omega_p < 100 cm^{-1} \Rightarrow \lambda_c > 15\ \mu m$

Resistivity of Tl-2201 Single Crystal

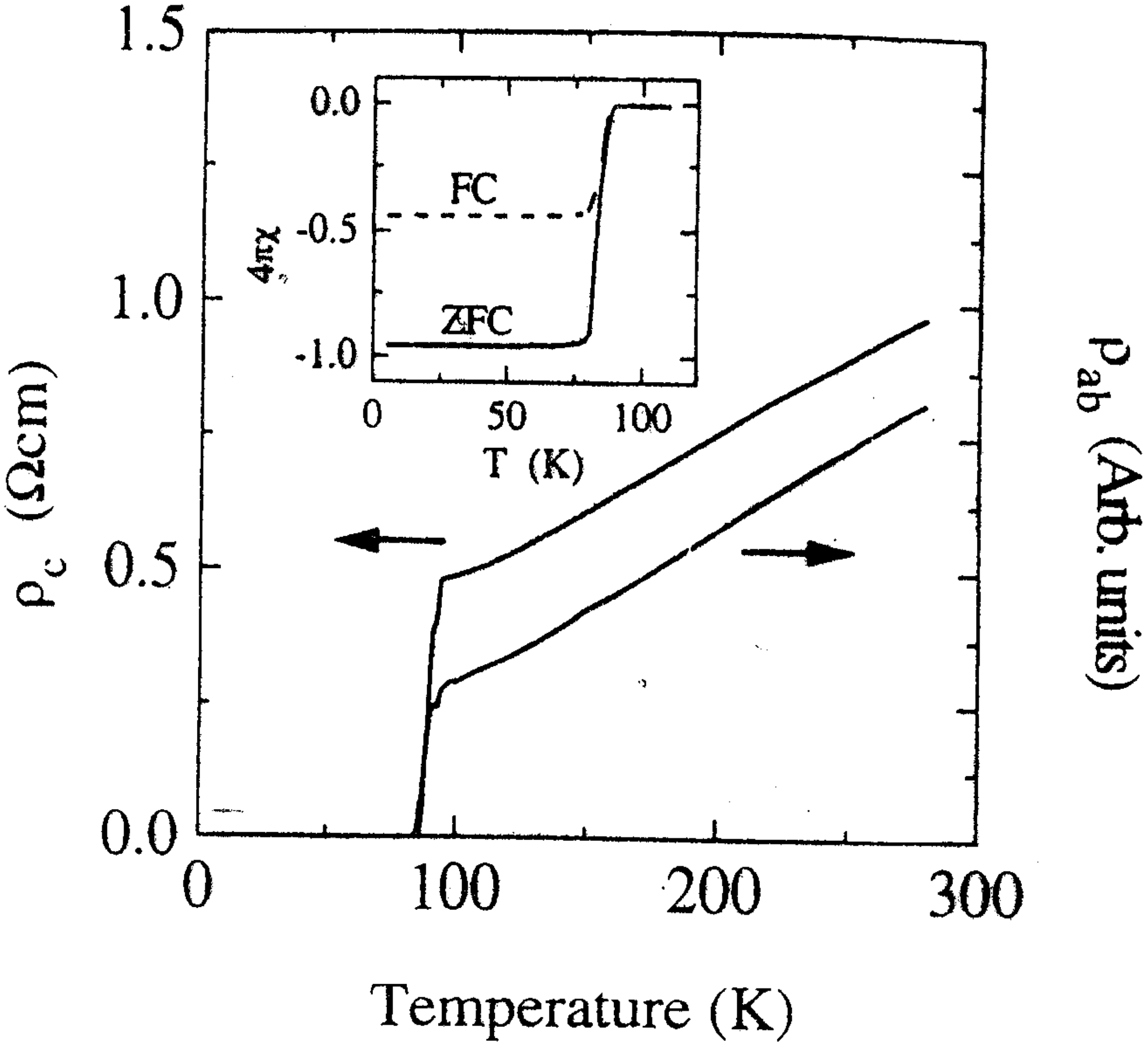

Schützmann et al, 1997.

18

Tl-2201 raw data

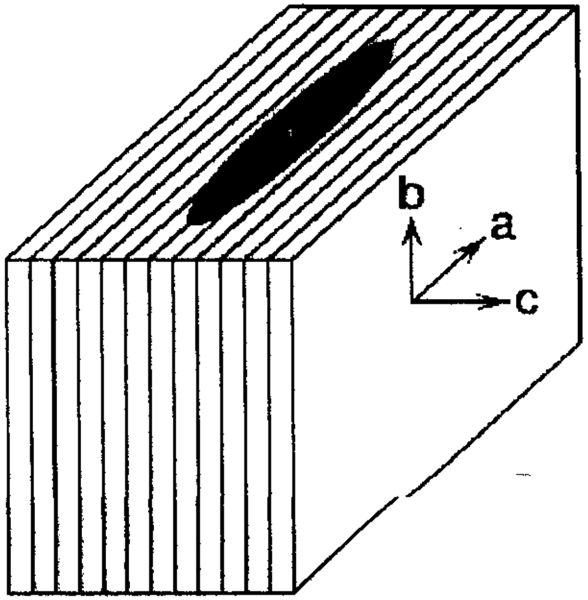

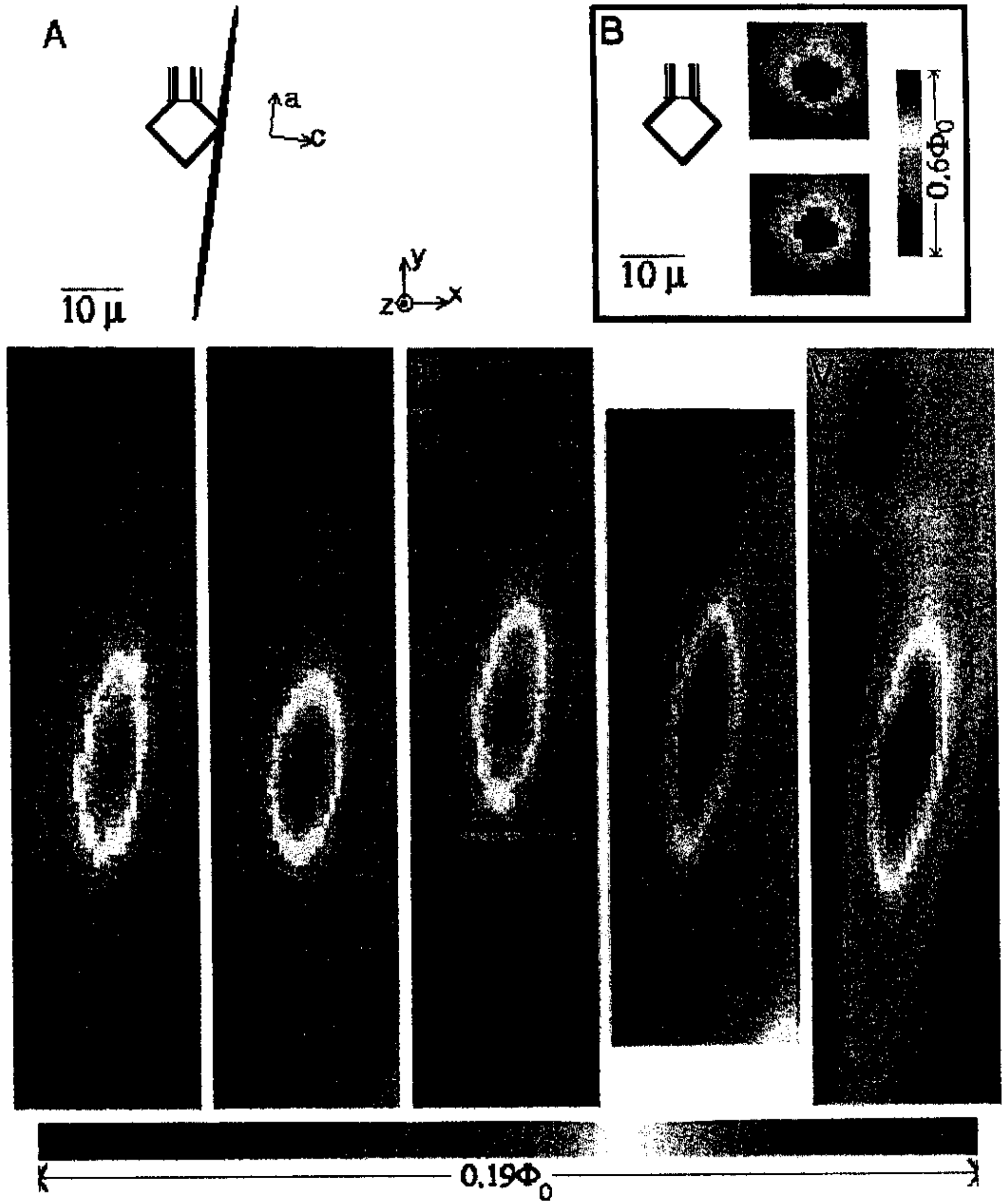

Quantitative Modeling

1st try — Full Width Half Maximum

2nd try — Neglect spreading below surface (wrong!) and integrate over SQUID pickup loop shape

$$b_z(x,y) = \frac{\Phi_0}{2\pi\lambda_{ab}\lambda_c} K_0\left(\sqrt{(s/2\lambda_{ab})^2 + (x/\lambda_{ab})^2 + (y/\lambda_c)^2}\right)$$

- propagate fields to height z_0
- integrate over pickup loop
- 2 free parameters: λ_c and z_0

3rd try (*Kogan and Clem*) — Solve the anisotropic London model at a superconductor-vacuum interface and integrate over the known SQUID pickup loop shape

$$b_z(x,y) = -\int k\varphi(k) e^{i\vec{k}\cdot\vec{r}-kz} \frac{d^2k}{(2\pi)^2}$$

where $$\varphi(\vec{k}) = \frac{-\Phi_0(1+m_1{k_x}^2)}{m_3\alpha_3(m_1{k_x}^2\alpha_3(k+\alpha_1)+k\alpha_3+{k_y}^2)}$$

and $\alpha_1 = \sqrt{\frac{1+m_1k^2}{m_1}}$ and $\alpha_3 = \sqrt{\frac{1+m_1{k_x}^2+m_3{k_y}^2}{m_3}}$

- evaluate integrals at height z_0
- integrate over pickup loop
- 2 free parameters: λ_c and z_0

caveat: Farid

(2)

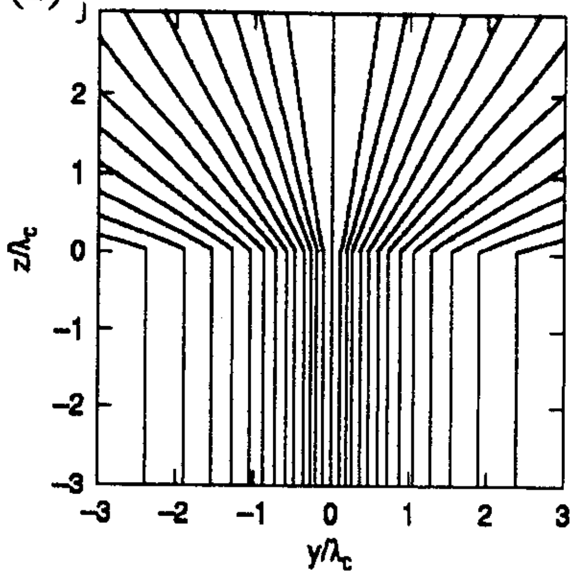

(3)

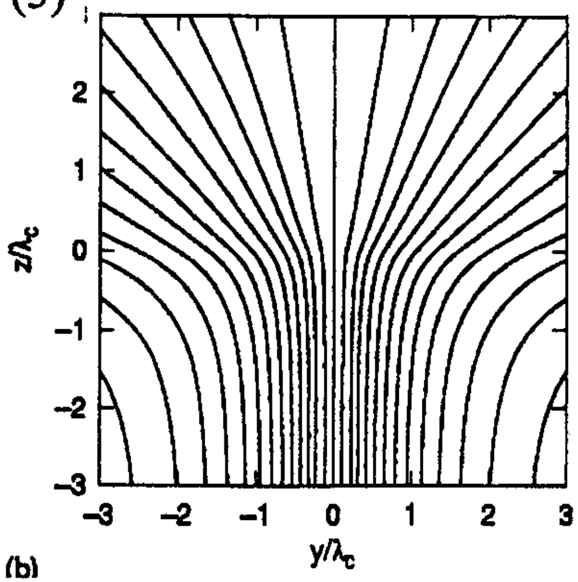

(b)

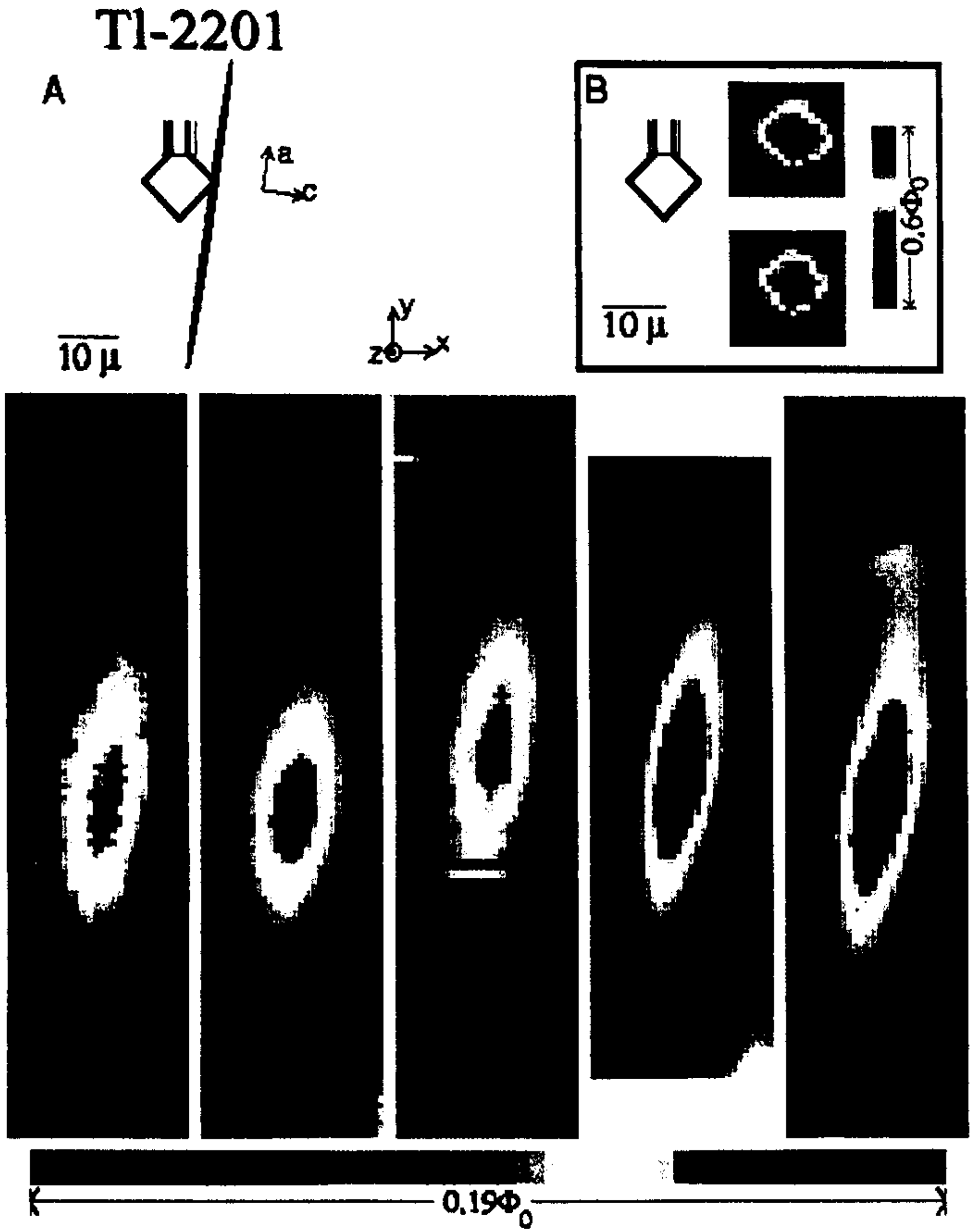

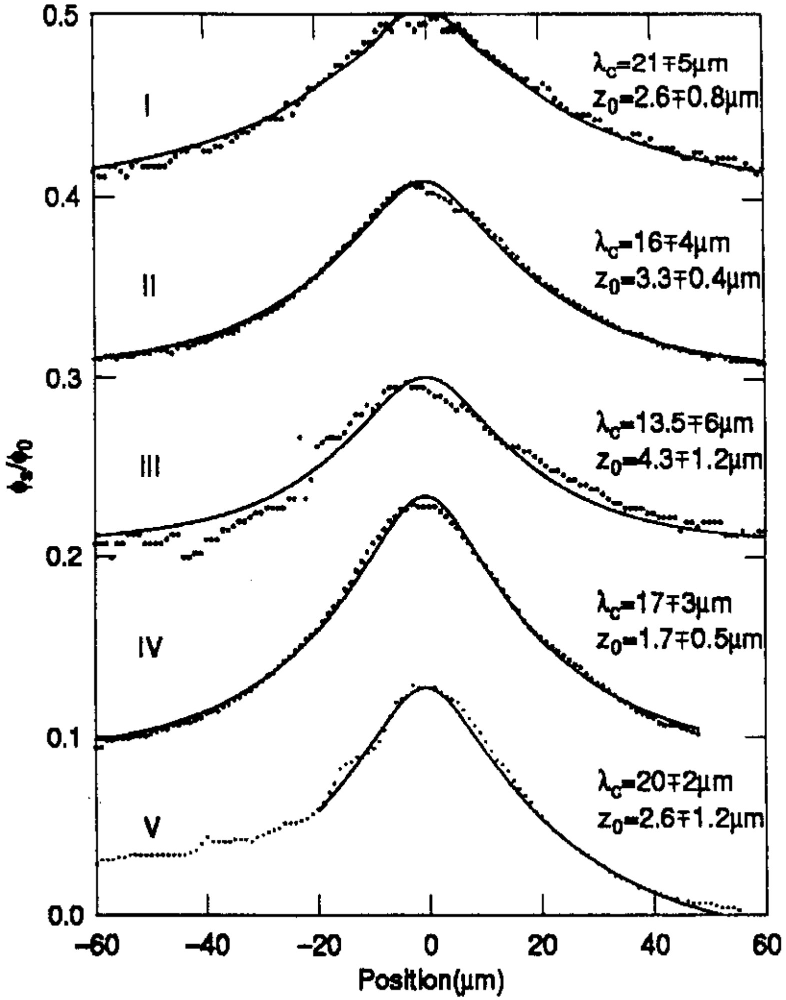

$\lambda_c \approx 18 \pm 3\ \mu m$

Are we measuring the intrinsic penetration depth in Tl-2201?

Vortices in 3 crystals from 2 groups gives consistent results with scanning SQUID microscopy.

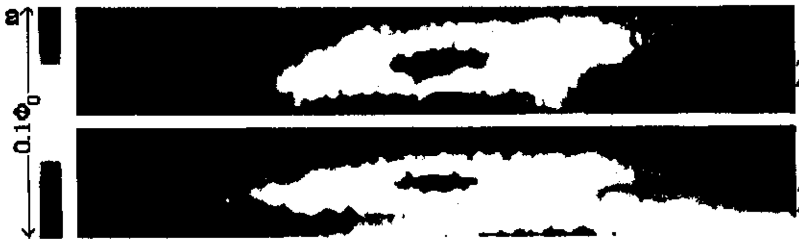

$\lambda c = 17 \pm 4\mu m$

$\lambda c = 19 \pm 1\mu m$

crystal from Kolesnikov

22

Optical techniques give consistent results.

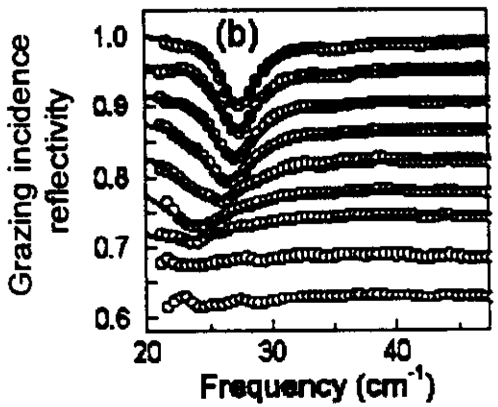

$\lambda c = 17\mu m$ Tsvetkov et al 1998 (thin films from Ren's group)

$\lambda c = 12\mu m$ Basov et al 1999 (crystals from Hinks)

No evidence for stacking faults or superlattice structure in TEM or x-ray.

$La_{2-x}Sr_xCuO_4$

$\lambda_c \approx 5 \pm 1\ \mu m$

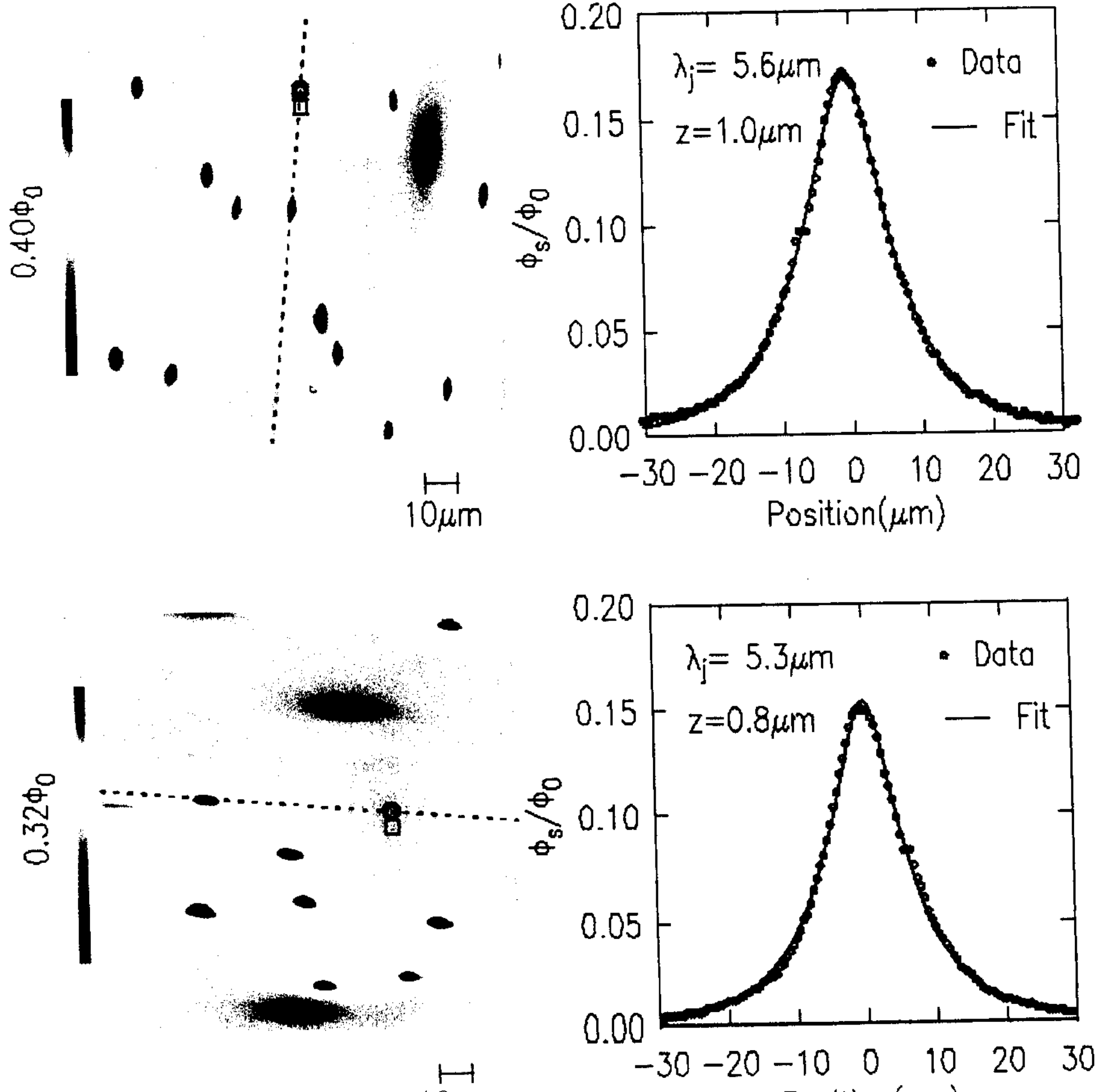

c-axis resistivity of $(Hg,Cu)Ba_2CuO_{4+\delta}$

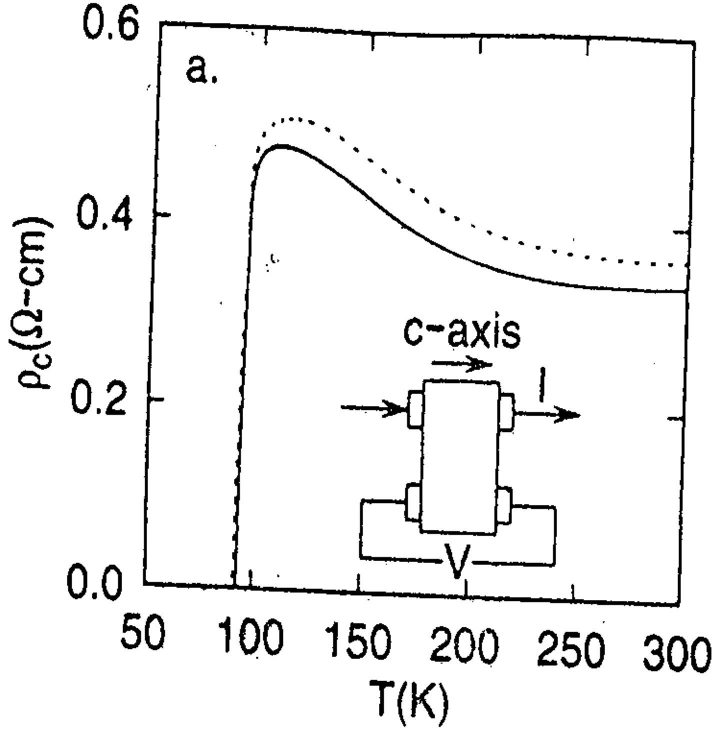

$(Hg,Cu)Ba_2CuO_{4+\delta}$

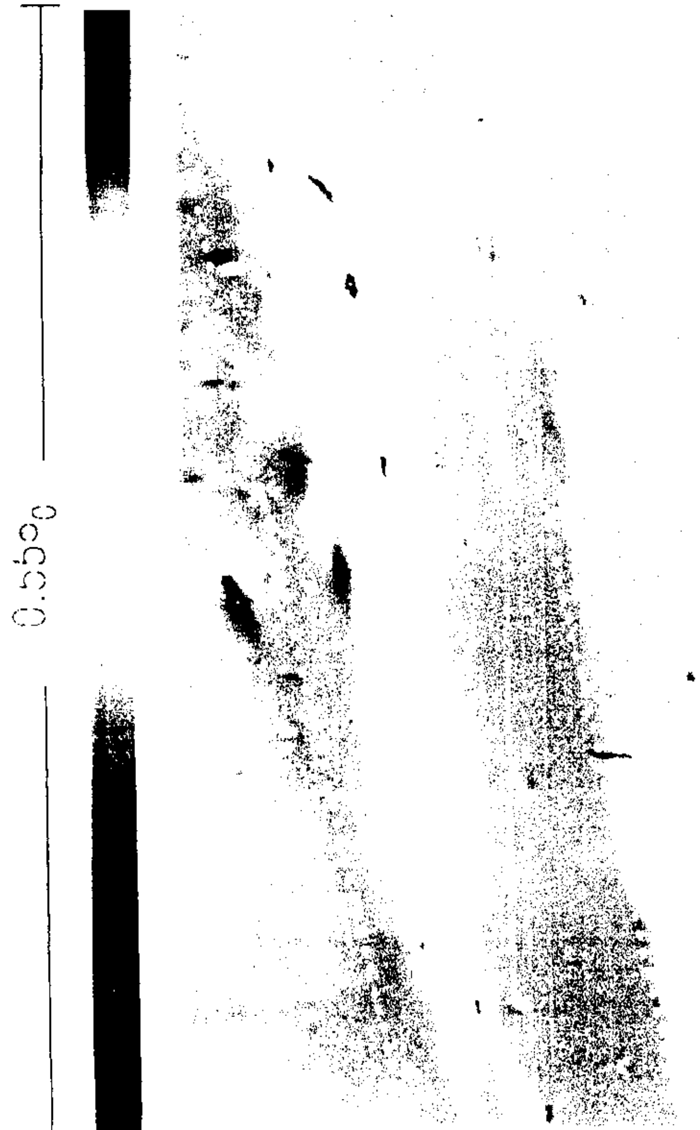

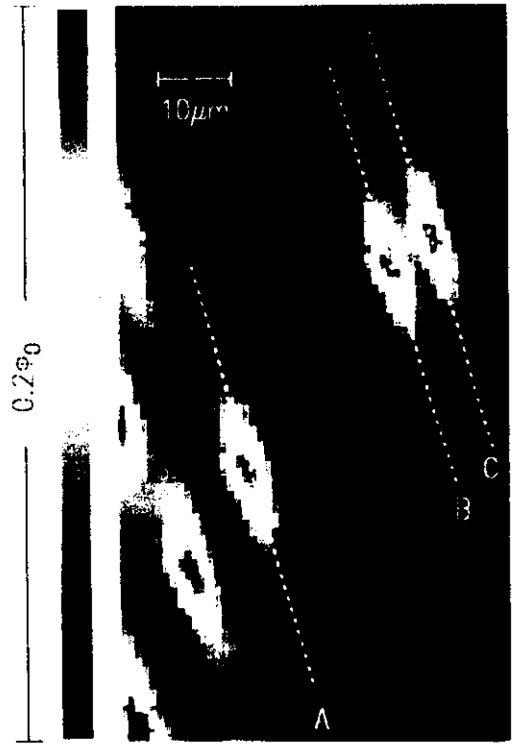

$\lambda_c \approx 8 \pm 1\ \mu m$

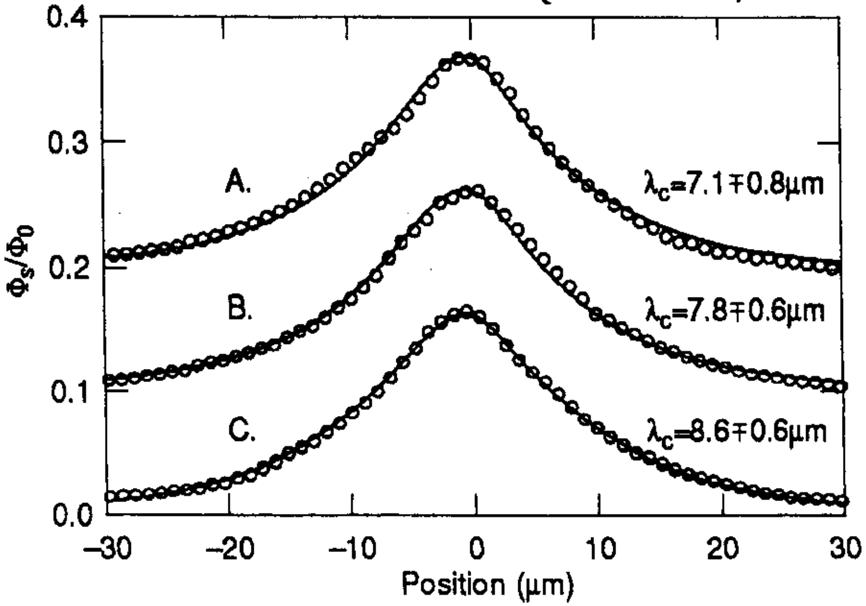

25

c-axis penetration depths in nominally optimally doped single-layer cuprates

	LSCO	Hg-1201	Tl-2201
λ_{ILT}	~3μm [Anderson*]	~1μm [Anderson†]	~1μm [Anderson*]
vortex imaging	~5μm [us]	8±1μm [us]	18±3μm [us]
optical (1/ω)	4½ μm [Uchida]	6μm [Basov]	12μm [Basov]
optical (sum rule)			
optical (ω_p)			17μm [van der Marel]
microwave	4 μm [Shibauchi]		
oriented powder susceptibility		1.36±0.16μm‡ [Panagopoulos]	
$\eta \approx \left(\frac{\lambda_{ILT}}{\lambda_c}\right)^2$	$\eta \approx 1$	$\eta \approx 10^{-2}$	$\eta \approx 10^{-3}$

*C_p by Loram
†C_p by Charalambous

‡slightly overdoped

The ILT mechanism can only supply 1% of the condensation energy in the two highest-Tc single-layer cuprates.

caveats

"Conventional" estimates for λ_c

Tl-2201

- Diffusive transmission — $\lambda_c \approx$ **1-6 μm**
  (parallel momentum not conserved)
- Diffusive + *d*-wave — $\lambda_c >$ 1–**6 μm**
  (or other anisotropic gap)
  Graf, Rainer, and Sauls
  Rojo and Levin
  Hirschfeld, Quinlan, and Scalapino
- Specular transmission — $\lambda_c \approx$ **1 μm**
  (parallel momentum conserved)
  Bulaevskii
- Das Sarma and Hwang — $\omega_p = 30\ \mathrm{cm}^{-1}$
  (elastic scattering, d-wave, realistic band structure)

Interlayer penetration depths

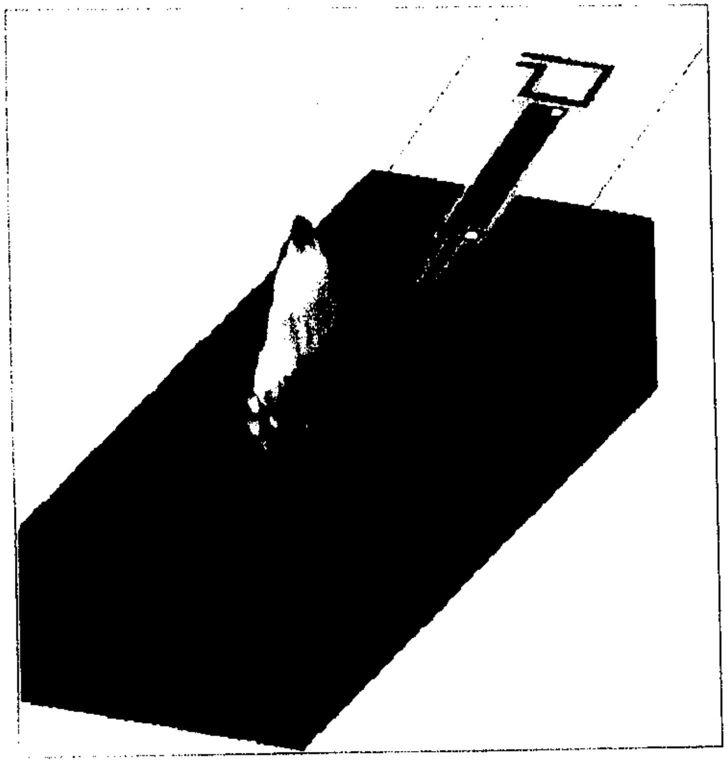

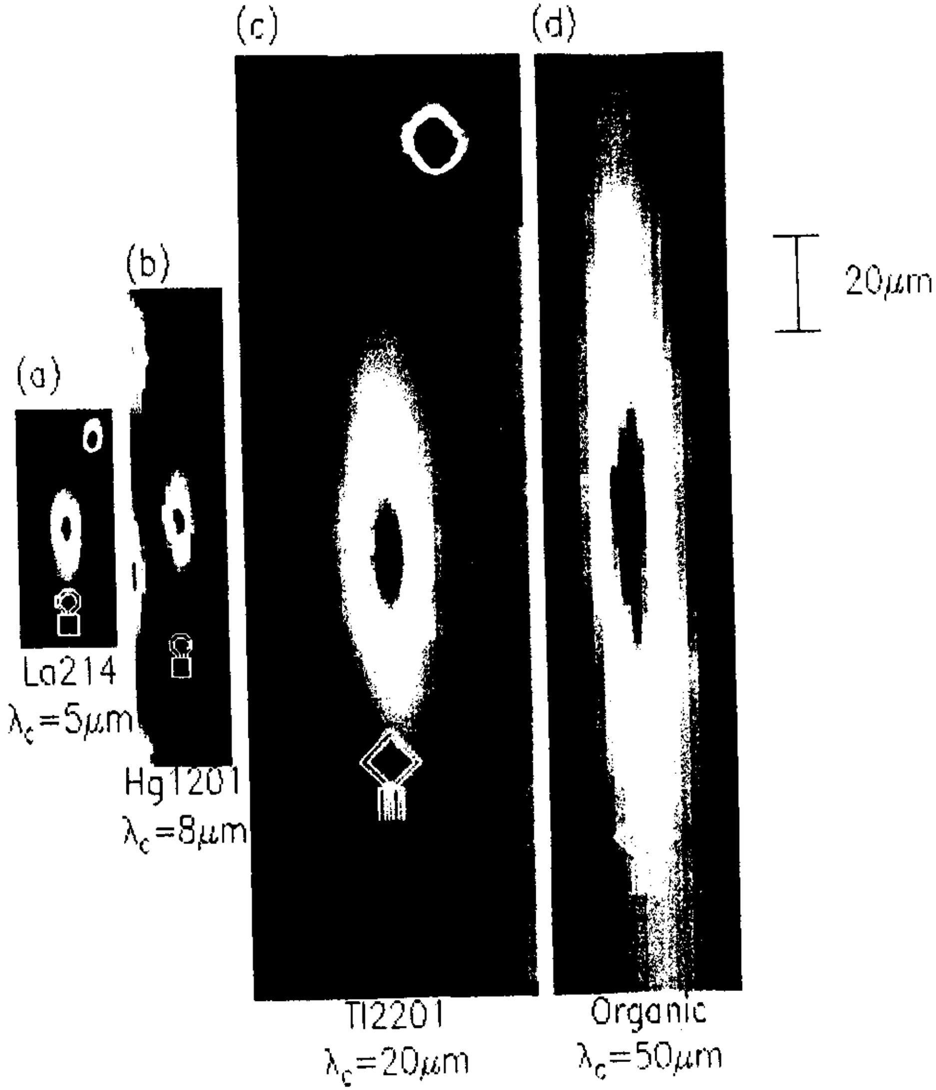

μ-SQUID Susceptometry

- Measurements of individual mesoscopic samples
- Local characterization of macroscopic samples

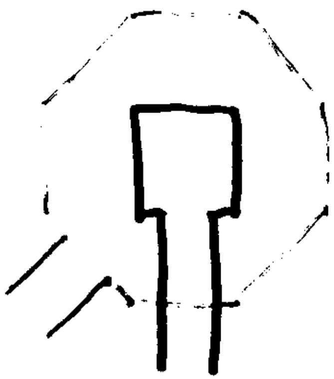

29

Scanning SQUID Susceptometry

30

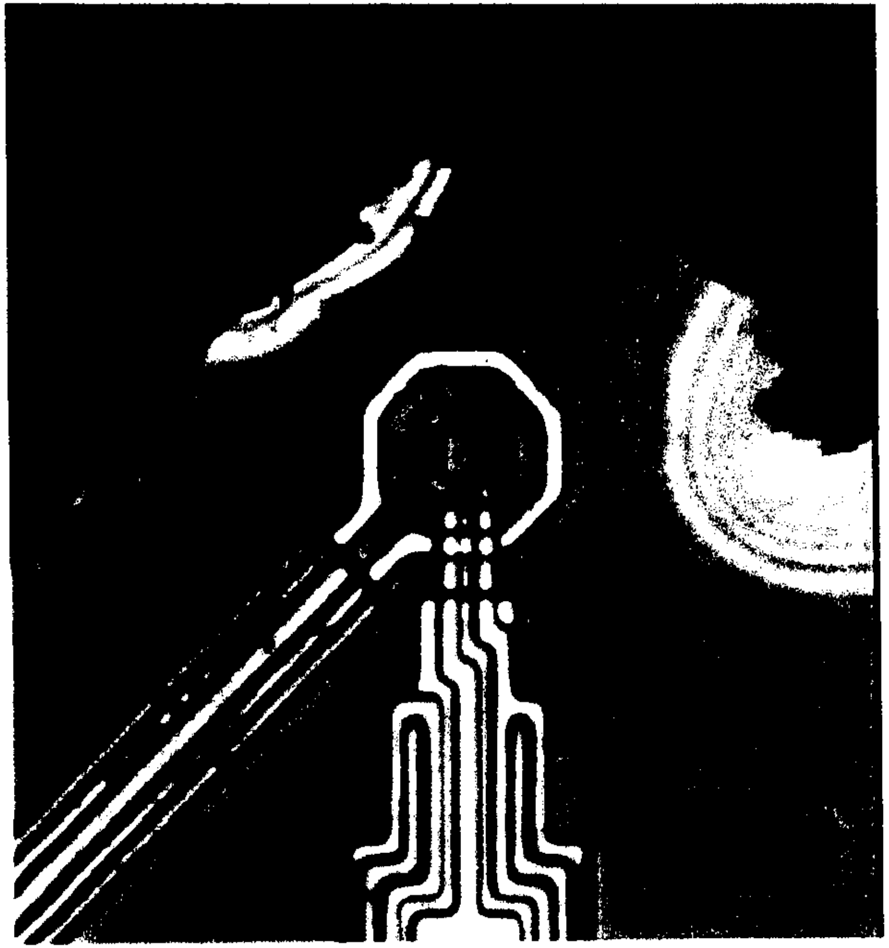

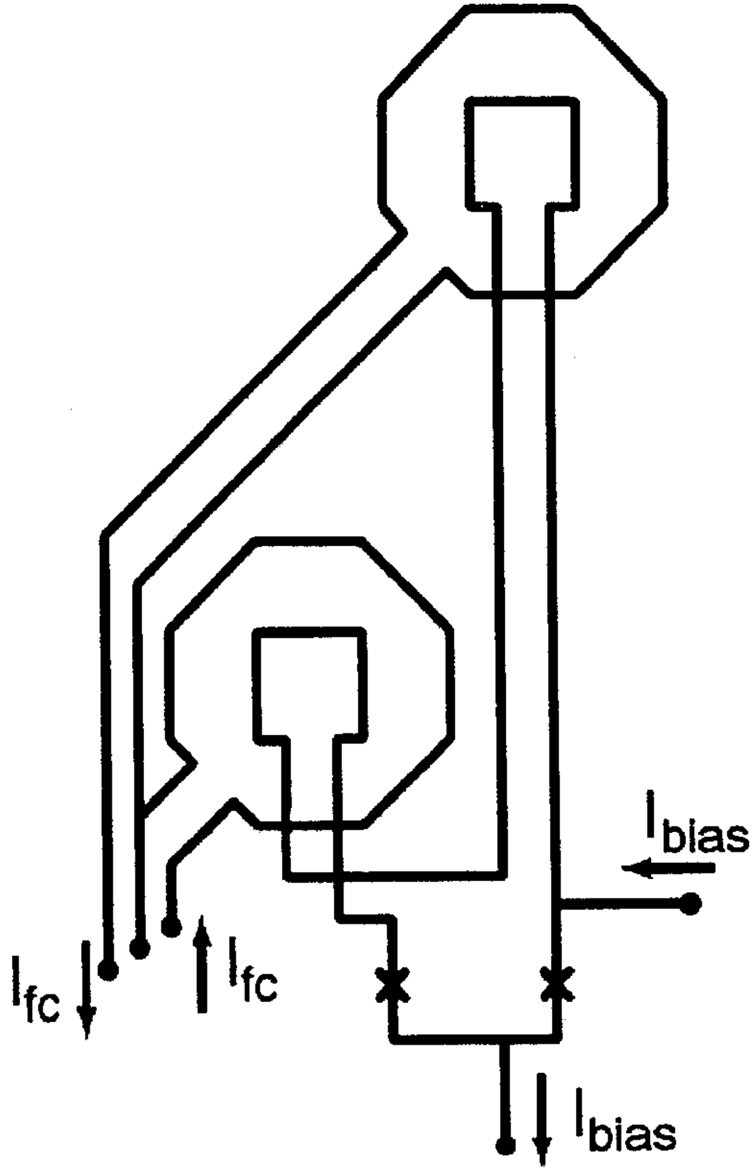

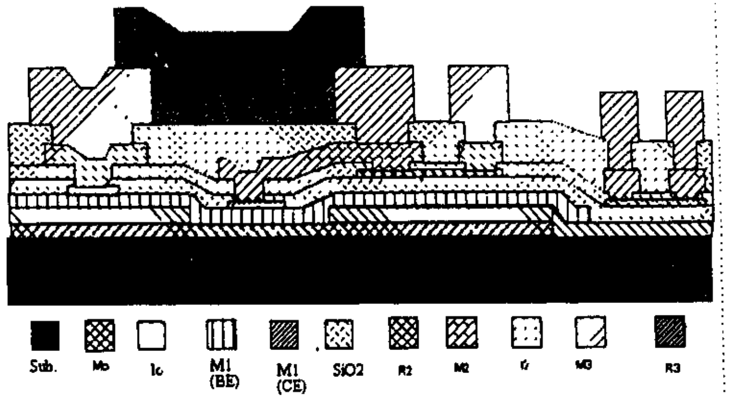

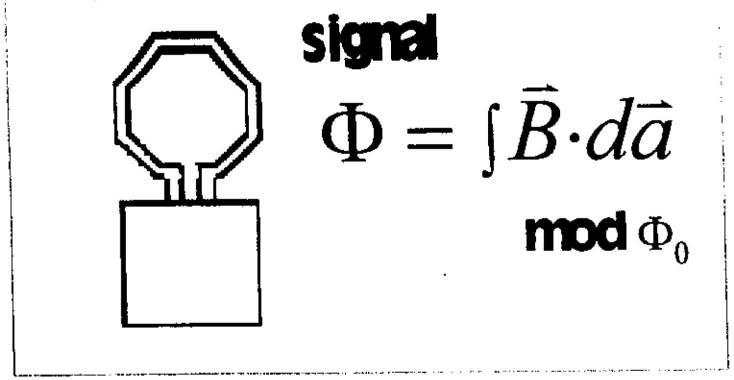

Nb SQUID Fabrication at HYPRES and SNF

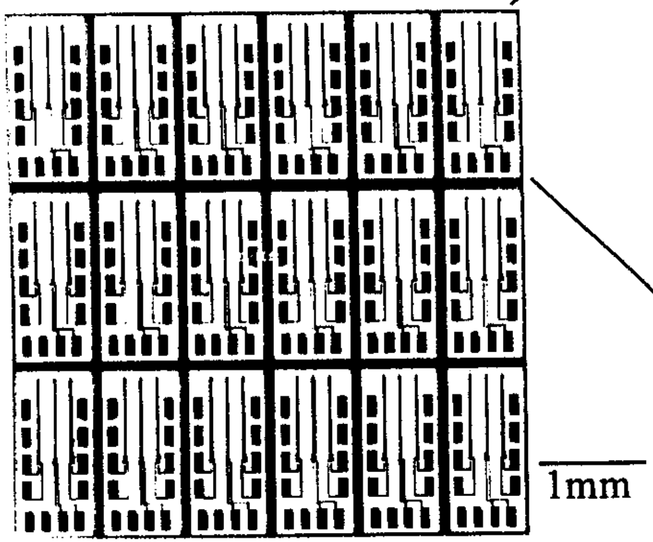

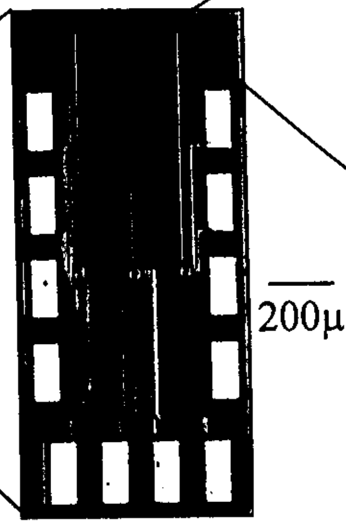

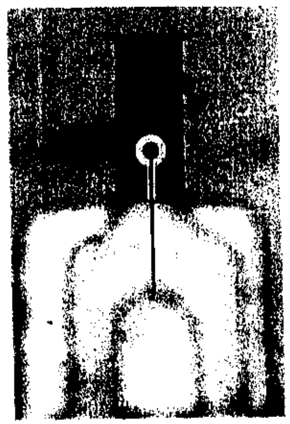

Final submicron etch at Stanford

SQUID Designs: IBM Joint Study Agreement
SNF Fabrication: Per Bjornsson, Adrian Lu

The Scanning Microscope

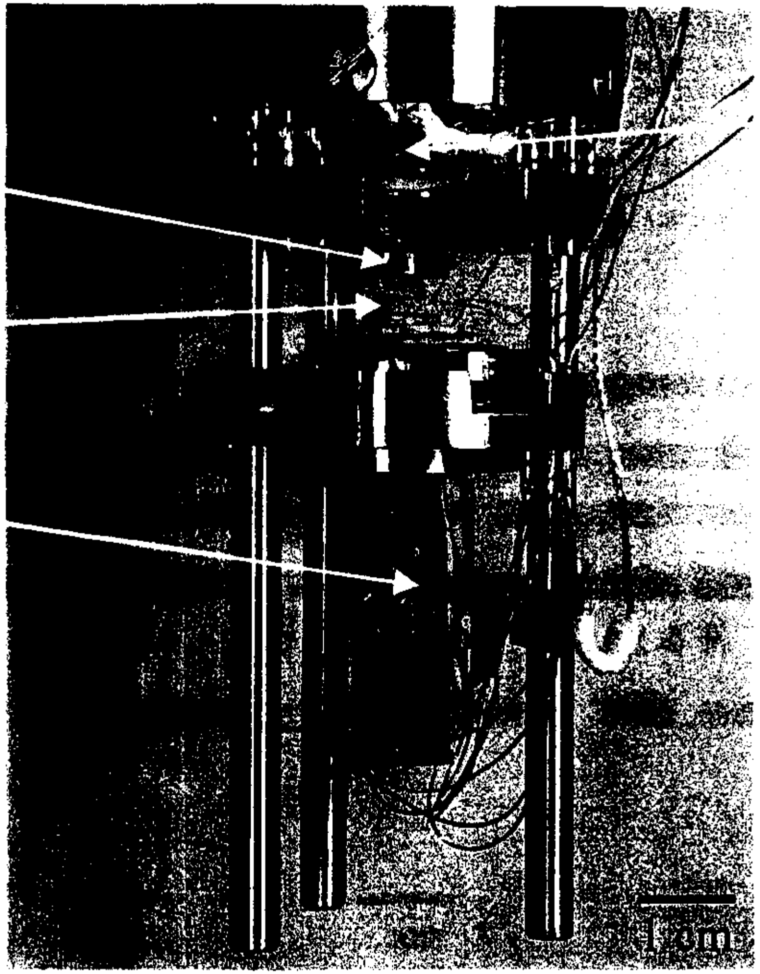

Large Area Scanner:

- **piezoelectric S-bender design**
- **70x70 μm^2 scan area at 4 K**
- **vib. noise ~ 1 Å**

Scanning SQUID

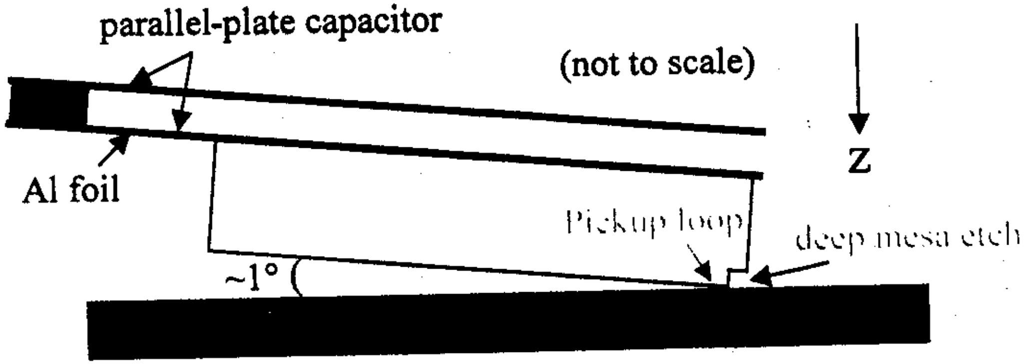

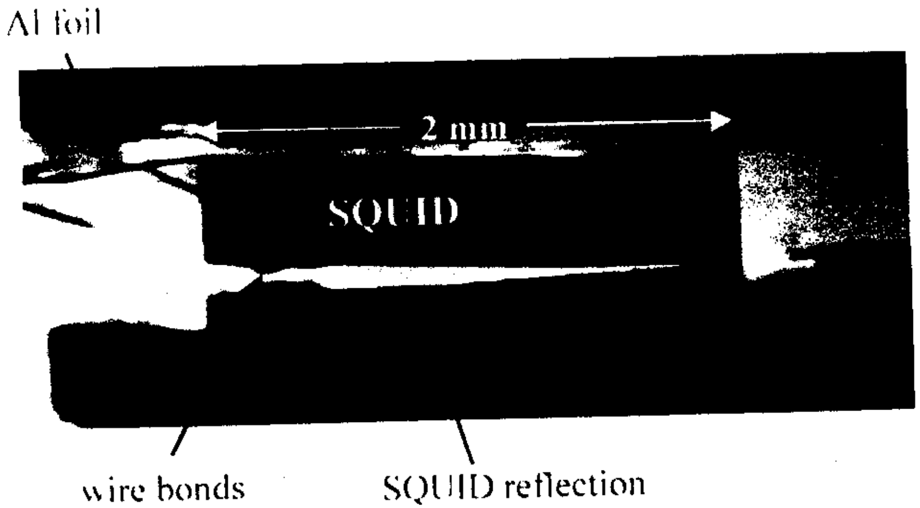

- **Pickup loop is approx. 3 μm above sample**
- **Capacitor provides Z information**

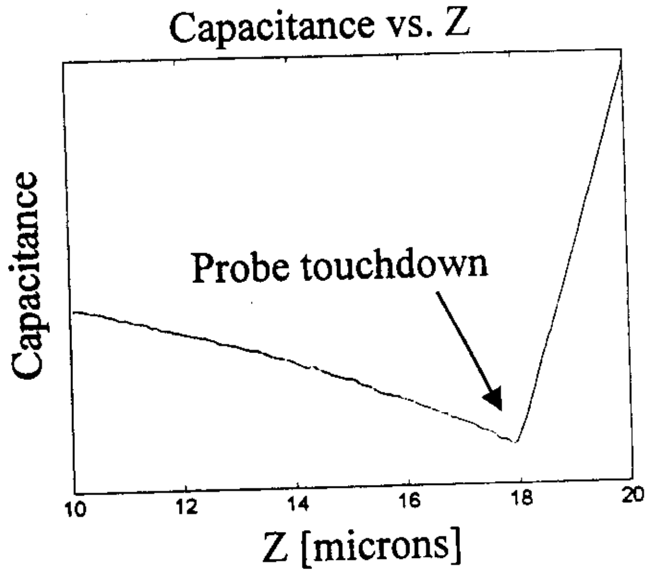

Image of an array of tin disks at 2.3K

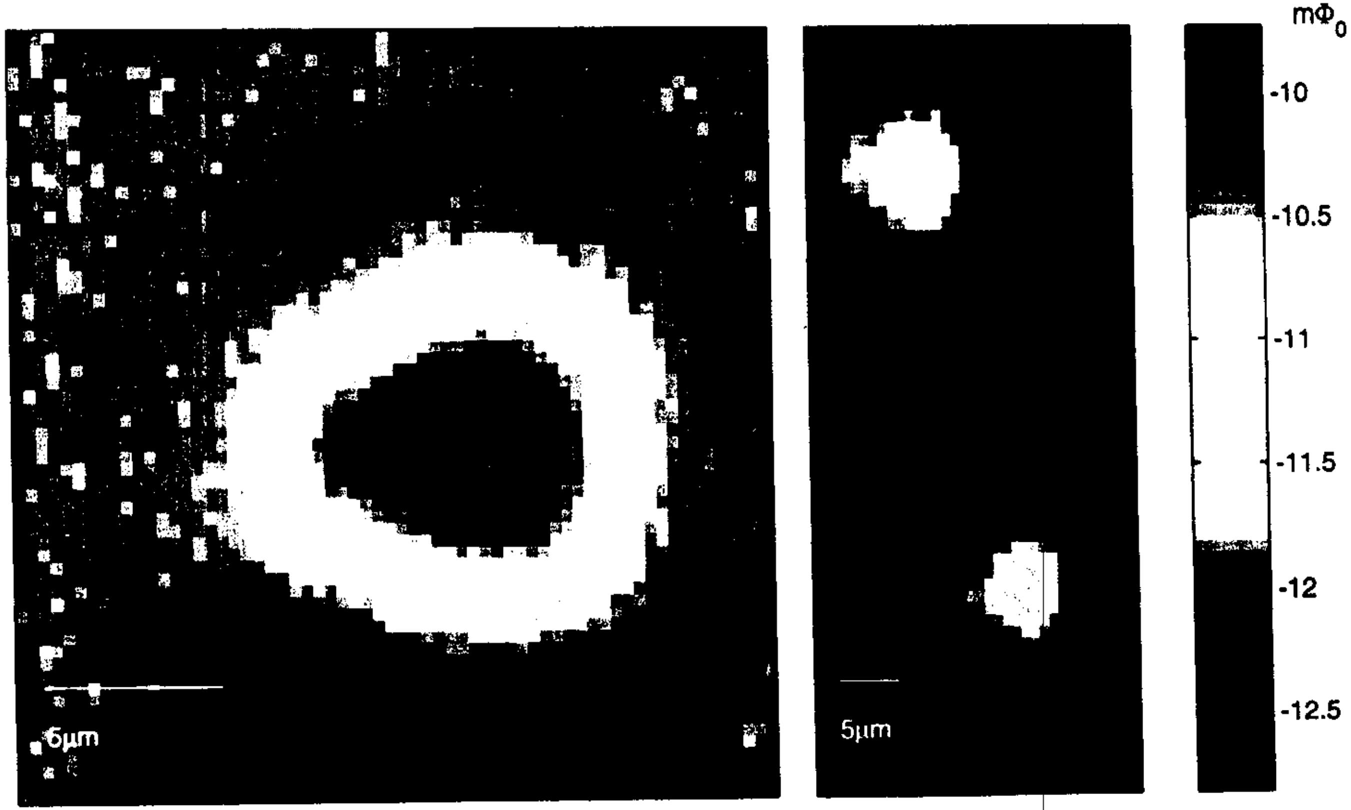

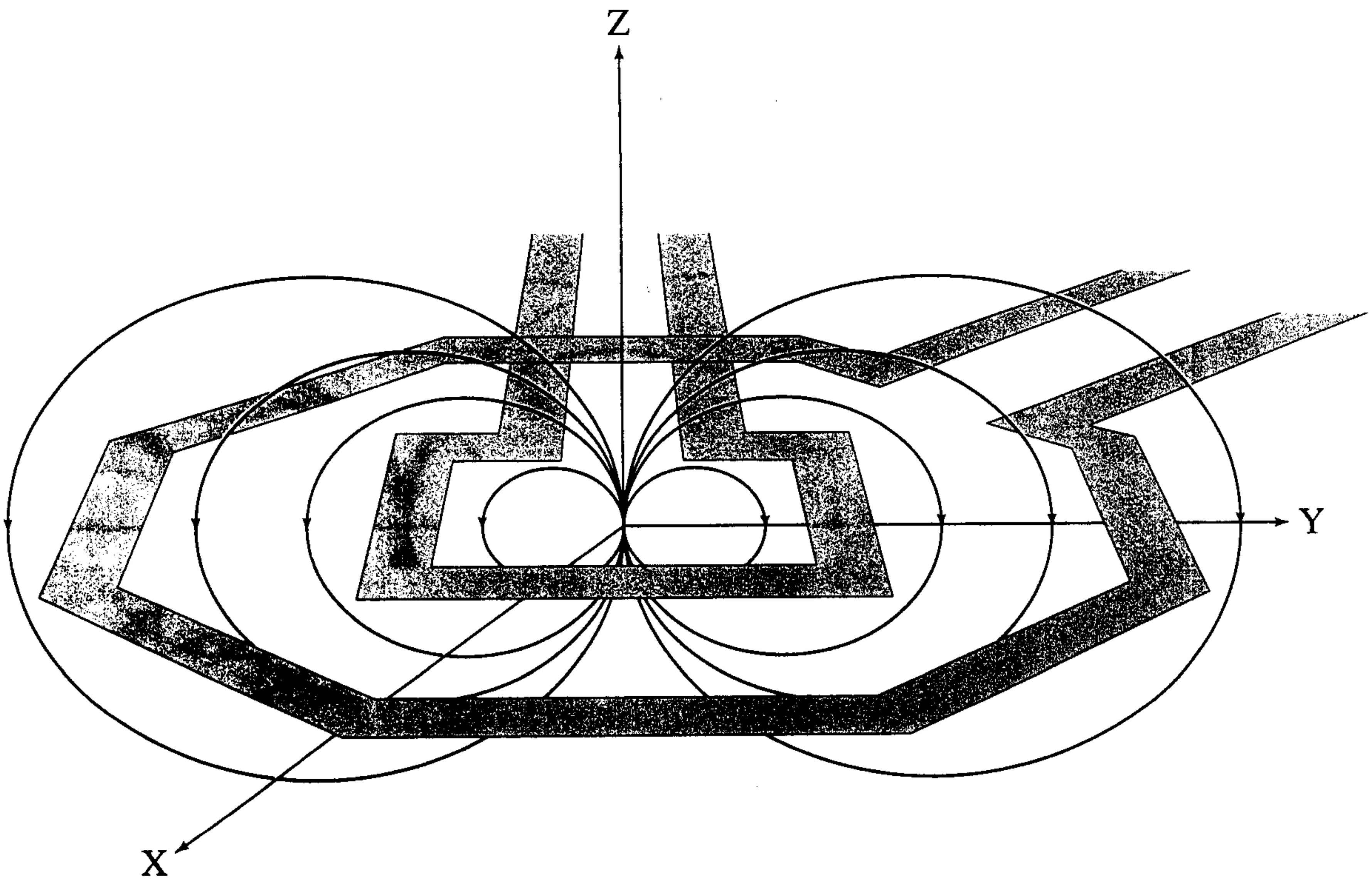
Z
Y
X

Image of a 3μ tin disk at 2.7 K

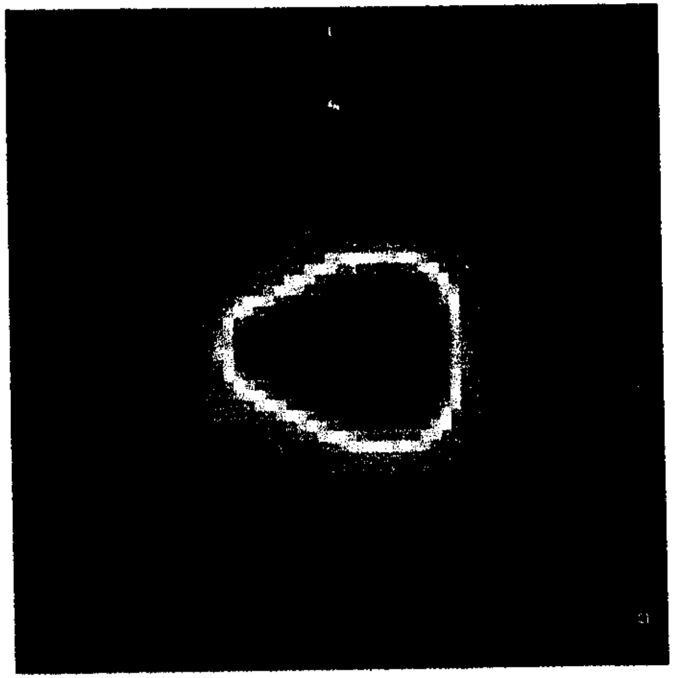

$I_a \approx 0.44\,mA$
$\Rightarrow H_a \approx 0.25\,G$

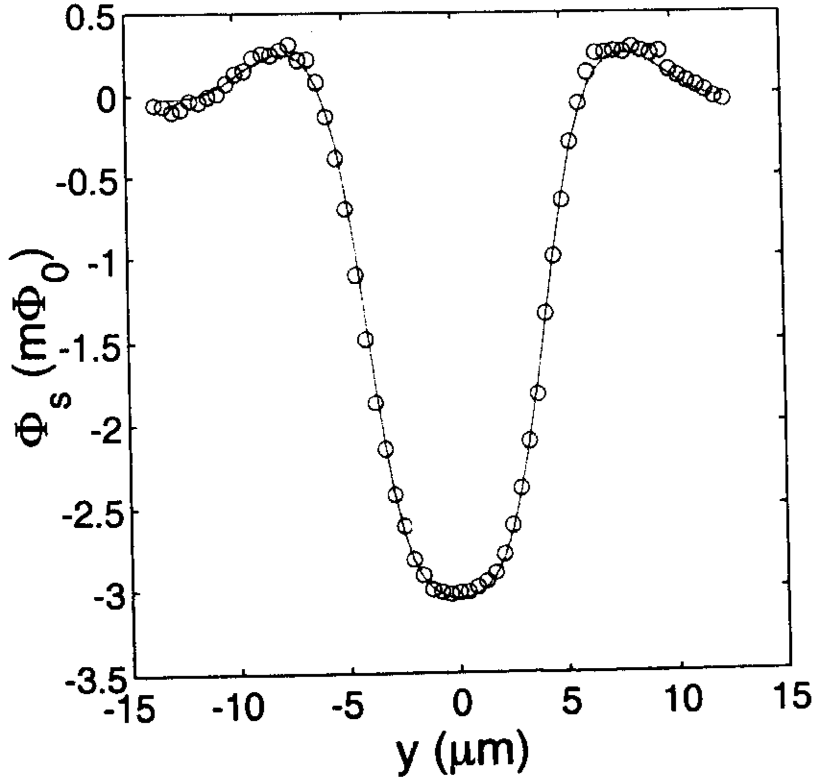

$$\frac{dm}{dH_a} = 3.65 * 10^7 \mu_B / G$$

min sensitivity $1 * 10^5 \mu_B / \sqrt{Hz}$

Scanning SQUID Susceptometry

- **Spin Sensitivity** $1\times10^{5}\ \mu_B/\sqrt{Hz}$

  Can be improved to $10^{3}\ \mu_B/\sqrt{Hz}$ with current sensors

  Can theoretically be improved to $1\ \mu_B/\sqrt{Hz}$ with subsequent generations

- **Spatial Resolution** $8\,\mu m$

  Can be improved to $\sim 0.5\,\mu m$ with subsequent generations.